Trace gas oxidizers are widespread and active members of soil microbial communities

Sean Bay, Xiyang Dong, James Bradley, Pok Man Leung, Rhys Grinter, Thanavit Jirapanjawat, Stefan Arndt, Perran Cook, Douglas Larowe, Philipp Nauer, et al.

1. Extended Data

Figure #	Figure title One sentence only	Filename This should be the name the file is saved as when it is uploaded to our system. Please include the file extension. i.e.: *Smith_ED Fig1.jpg*	Figure Legend If you are citing a reference for the first time in these legends, please include all new references in the Online Methods References section, and carry on the numbering from the main References section of the paper.
Extended Data Fig. 1	Composition of the bacterial and archaeal communities sequenced in each soil metagenome.	Extended-Data-Figure-1.tif	Stacked barcharts depicting the relative abundance of different phyla in **(a)** Australian soils and **(b)** global soils based on reads for the single-copy ribosomal protein gene *rplP*. Alpha diversity is shown as observed and estimated richness (Chao1) in **(c)** Australian soils and **(d)** global soils. Boxplots show median, lower and upper quartile, and minimum and maximum values. This is based on four biological replicates for the four Australian soils (n = 16) at depths of 0-5, 5-10, 15-20, and 25-30 cm, and biological triplicates for the eight global soils (n = 24). For beta diversity, abundance-based distance matrix Bray-Curtis diversity is visualized on a multidimensional PcoA plot for both Australian and global soils. Testing for significant differences in community structure between depths and ecosystems was performed using a one-way PERMANOVA with 999 permutations.
Extended Data Fig. 2	Metatranscriptomic analysis comparing metabolic marker gene expression across three	Extended-Data-Figure-2.tif	**(a)** Relative abundance of quality-filtered metatranscriptomic short reads expressed as the total reads per kilobase per million (RPKM). **(b)** Relative abundance of genes in each metatranscriptome mapped to the corresponding assemblies

	global soils with paired metagenome and metatranscriptome datasets.		from each soil expressed as total transcripts per million (TPM).
Extended Data Fig. 3	Analysis of aerobic methane oxidation enzymes and pathways in sampled soils.	Extended-Data-Figure-3.tif	**(a)** Maximum-likelihood tree of amino acid sequences of particulate methane monooxygenase A subunit (PmoA), a marker for aerobic methane oxidation. The tree shows 2 sequences from soil metagenome-assembled genomes (blue) and 12 sequences from unbinned contigs (red) alongside 93 representative sequences from NCBI reference genomes (black). The tree shows the affiliation of the PmoA from *Candidatus* Methylotropicum kingii with those of amplicons of the tropical upland soil cluster (TUSC). Also shown are reference sequences of other members of the copper membrane monooxygenase superfamily, namely ammonia monooxygenase (AmoA), hydrocarbon monooxygenase (HmoA), and groups of unknown function (including PxmA). The tree was constructed using the JTT matrix-based model, used all sites, and was bootstrapped with 50 replicates and midpoint-rooted. Source data is provided in Newick (nwk) format. **(b)** Metabolic reconstruction of the putative novel methanotroph *Candidatus* Methylotropicum kingii. The core pathways associated with energy conservation and carbon acquisition are shown, with genes detected shown in italics. The bacterium is predicted to use methane, methanol, and acetate as energy and carbon sources. In addition, it can use molecular hydrogen as an electron donor via a group 1f [NiFe]-hydrogenase. The bacterium is predicted to use the electron acceptors oxygen *via* a cytochrome *c* oxidase and nitrous oxide *via* a nitrous oxide reductase. Its particulate methane monooxygenase forms a distinct phylogenetic lineage with amplicons from the Tropical Upland Soil Cluster (TUSC), whereas its methanol dehydrogenase is closely related to those in previously sequenced Gemmatimonadota MAGs inferred to be methylotrophic. The genome encodes key

			enzymes for the serine cycle for assimilation of one-carbon sources. Abbreviations: H_4F = tetrahydrofolate; Hyd = group 1f [NiFe]-hydrogenase; pMMO = particulate methane monooxygenase; MDH = methanol dehydrogenase; PQQ = pyrroloquinoline quinone; I = NADH dehydrogenase (complex I); II = succinate dehydrogenase (complex II); IV = cytochrome aa_3 oxidase (complex IV). Dashed black lines indicate diffusion. Dashed gray lines indicate unknown process or undetected genes. **(c)** Molecular model of the putative particulate methane monooxygenase (Pmo) from *Candidatus* Methylotropicum kingii and comparison with putative catalytic sites of other experimentally validated Pmos. (i) Molecular model of the functional homotrimer of the putative Pmo complex from *Ca.* M. kingii, shown as a cartoon representation. PmoA, PmoB, and PmoC subunits from one Pmo complex are colored in light blue, dark blue, and sky blue respectively. The other two Pmo complexes in the trimer are colored in transparent yellow. Cu ions bound in the putative active site of the color-coded Pmo complex are shown as ochre spheres. TM = transmembrane. (ii) Zoomed view of the Pmo complex from panel A, with the three Pmo subunits labelled and the putative active sites Cu_B and Cu_C highlighted. (iii) Stick representation of residues in the Cu_B and Cu_C active sites of Pmo molecular models from *Ca.* M. kingii (Gemmatimonadota) and *Methylacidiphilum infernorum* (Verrucomicrobiota), and from the crystal structure (PDB ID: 3RGB) of Pmo from the *Methylococcus capsulatus* (Proteobacteria), showing that both sites are conserved between Pmo from *Ca.* M. kingii and *M. capsulatus*. Pmo from *M. infernorum* lacks the Cu_B site, suggesting this site is not responsible for methane oxidation. (iv) Sequence alignment of metal binding motifs from the Cu_B (left) and Cu_C (right) sites from Pmo from *Ca.* M. kingii (*cMk.*), *M. capsulatus* (*Mc.*), *Candidatus* Methylomirabilis limnetica (*cMl.*; Methylomirabilota), and *M. infernorum* (*Mi.*). Amino acids involved in Cu coordination are highlighted.

Extended Data Fig. 4	Biogeochemical measurements of *in situ* soil gas concentrations and validation of static chamber setup.	Extended-Data-Figure-4.tif	**(a)** Mean soil-gas profiles normalized to the respective ambient air concentration (dashed line) of four biological replicates collected at depths of 0, 2, 4, 6, 8, 10, and 16 cm across four Australian ecosystems (n = 112). Note that the different gases were sampled at identical depths, but points are plotted slightly offset on the y-axis for better visibility of error bars. **(b)** Laboratory static chamber incubations (n = 3) to control for abiotic release of trace gases from chamber's plastic components. Chamber headspace mixing ratios of hydrogen (H_2), carbon monoxide (CO), and methane (CH_4) were measured at eight time points during ~25 minutes of incubation time of an inert stainless steel surface. Measurement setup, sampling procedure, and sampling frequency followed those applied during the *in situ* chamber incubations performed to measured soil-atmosphere flux of trace gases. Circles indicate mixing ratio averaged from three independent incubations, with the vertical lines denoting one standard deviation. Dashed lines indicate the mixing ratio of trace gas averaged across three air samples.
Extended Data Fig. 5	Maximum-likelihood tree of amino acid sequences of group 3 [NiFe]-hydrogenase large subunits, a marker for hydrogen production during fermentation processes.	Extended-Data-Figure-5.tif	The tree shows 129 sequences from soil metagenome-assembled genomes (blue) alongside 172 representative sequences from NCBI reference genomes (black). The subgroup of each reference sequence is denoted according to the HydDB classification scheme [41]. The tree was constructed using the JTT matrix-based model, used all sites, and was bootstrapped with 50 replicates and midpoint-rooted. All sequences shorter than 350 amino acids were omitted. Source data is provided in Newick (nwk) format.
Extended Data Fig. 6	Gas chromatography studies of one *ex situ* trace gas consumption experiment.	Extended-Data-Figure-6.tif	Shown are four biological replicates collected at depths of 0-5, 5-10, 15-20, and 25-30 cm across four Australian ecosystems (n = 64). Depicted are the oxidation rates recorded over time of **(a)** atmospheric H_2, **(b)** atmospheric CO, and **(c)** atmospheric CH_4 by soils at each depth compared to heat-

			killed control soils. Oxidation of the three gases was also measured in the dryland soils following hydration, i.e. Dryland (wet) samples. Points show average values and vertical lines the error bars representing one standard deviations of four biological replicates. Significance testing of differences in *ex situ* oxidation rates between ecosystem type and soil depth was carried out using a one-sided Kruskall Wallis H test followed by a pairwise Wilcoxon tests with adjusted *p*-values using a Benjamini Hochberg correction for multiple testing. Boxplots show median, lower and upper quartile, and minimum and maximum values comparing the *ex situ* rates of H_2, CO, and CH_4 oxidation between depths and ecosystems for **(d)** cell-specific rates and **(e)** bulk reaction rates per gram of dry soil.
Extended Data Fig. 7	Copy number of the 16S rRNA gene per gram of soils of four biological replicates.	Extended-Data-Figure-7.tif	Soil samples were collected at depths of 0-5, 5-10, 15-20, and 25-30 cm across four Australian ecosystems, with four biological replicates for each depth (n = 64). Boxplots show median, lower and upper quartile, and minimum and maximum values.
Extended Data Fig. 8	Comparison of the theoretical and measured population of trace gas oxidizers in soils,	Extended-Data-Figure-8.tif	Shown are four biological replicates collected at depths of 0-5, 5-10, 15-20, and 25-30 cm across four Australian ecosystems (n = 64). The theoretical populations, in line with the methods of Conrad [69], were estimated from thermodynamic modeling and measured *ex situ* oxidation rates assuming a single maintenance energy for all cells. Two different values were used: 8.9×10^{-15} W cell^{-1} as assumed by Conrad [69] and 1.9×10^{-15} W cell^{-1} as the median of metabolic rates reported by DeLong et al [61]. The measured populations of trace gas oxidizers were determined from 16S rRNA gene copy numbers and the relative abundance of the respective functional gene as determined from metagenomics. The ratio of theoretical vs. measured population is equivalent to dividing our calculated power per cell by the respective maintenance energy above. Boxplots show median, lower and upper quartile, and

			minimum and maximum values.
Extended Data Fig. 9	Maximum-likelihood tree of amino acid sequences of ribulose 1,5-bisphosphate carboxylase / oxygenase (RbcL), a marker for carbon fixation through the Calvin-Benson cycle.	Extended-Data-Figure-9.tif	The tree shows 68 sequences from soil metagenome-assembled genomes (blue) alongside 126 representative sequences from NCBI reference genomes (black). The subtype of each reference sequence is denoted. The tree was constructed using the JTT matrix-based model, used all sites, and was bootstrapped with 50 replicates and midpoint-rooted. Source data is provided in Newick (nwk) format.
Extended Data Fig. 10	Summary of the processes and mediators of trace gas cycling at the soil-atmosphere interface.	Extended-Data-Figure-10.tif	The soil bacterial phyla capable of consuming the trace gases H_2 (*via* group 1 and 2 [NiFe]-hydrogenases), CO (*via* form I carbon monoxide dehydrogenases), and CH_4 (*via* particulate methane monooxygenases) are shown. They are listed in order of the number of metagenome-assembled genomes recovered (black for highly abundant and grey for less abundant trace gas oxidizers). The downward arrows show the net consumption of atmospheric H_2, CO, and CH_4 by soil bacteria. The upward arrows show processes that result in endogenous production and internal cycling of trace gases. The green boxes indicate biotic processes, whereas the brown boxes indicate abiotic processes.

2. Supplementary Information:

A. Flat Files

Item	**Present?**	**Filename** **This should be the name**	**A brief, numerical description of file contents.** **i.e.:** ***Supplementary Figures 1-4, Supplementary Discussion, and***

		the file is saved as when it is uploaded to our system, and should include the file extension. The extension must be .pdf	***Supplementary Tables 1-4.***
Supplementary Information	Yes	Supplementary information.pdf	Supplementary Tables 1 to 12 Supplementary Figures 1 to 10
Reporting Summary	Yes	AB Rep Summary.pdf	
Peer Review Information	Yes	Greening_TPR File.pdf	

B. Additional Supplementary Files

Type	**Number** **If there are multiple files of the same type this should be the numerical indicator. i.e. "1" for Video 1, "2" for Video 2, etc.**	**Filename** **This should be the name the file is saved as when it is uploaded to our system, and should include the file extension. i.e.: *Smith_ Supplementary Video 1.mov***	**Legend or Descriptive Caption** **Describe the contents of the file**
Supplementary Table		Supplementary Tables 1-12.xlsx	Supplementary Tables 1 to 12 in XLSX format.
Supplementary Data		Phylogenetic tree newick files.zip	Raw phylogenetic trees in NWK format for Figures 2a, 2b, ED Figure 3, ED Figure 5, ED Figure 9, and Supplementary Figures 1 to 10.

17 # 3. Source Data

18

Figure	**Filename** **This should be the name the file is saved as when it is uploaded to our system, and should include the file extension. i.e.: *Smith_Source Data Fig1.xls,* or *Smith_ Unmodified Gels_Fig1.pdf***	**Data description** **i.e.: Unprocessed Western Blots and/or gels, Statistical Source Data, etc.**
Source Data Fig. 1	Source Data Fig 1.xlsx	Numerical source data
Source Data Fig. 3	Source Data Fig 3.xlsx	Numerical source data
Source Data Extended Data Fig. 1	Source Data Extended Data Fig 1.xlsx	Numerical source data
Source Data Extended Data Fig. 2	Source Data Extended Data Fig 2.xlsx	Numerical source data
Source Data Extended Data Fig. 4	Source Data Extended Data Fig 4.xlsx	Numerical source data
Source Data Extended Data Fig. 6	Source Data Extended Data Fig 6.xlsx	Numerical source data
Source Data Extended Data Fig. 7	Source Data Extended Data Fig 7.xlsx	Numerical source data
Source Data Extended Data Fig. 8	Source Data Extended Data Fig 8.xlsx	Numerical source data

Trace gas oxidizers are widespread and active members of soil microbial communities

Sean K. Bay[1,2], Xiyang Dong[3], James A. Bradley[4,5], Pok Man Leung[1,2], Rhys Grinter[2], Thanavit Jirapanjawat[1,2], Stefan K. Arndt[6], Perran L.M. Cook[7], Douglas LaRowe[8], Philipp A. Nauer[7], Eleonora Chiri[1,2 *], Chris Greening[1,2 *]

[1]School of Biological Sciences, Monash University, Clayton, VIC 3800, Australia

[2]Department of Microbiology, Biomedicine Discovery Institute, Monash University, Clayton, VIC 3800, Australia

[3]School of Marine Sciences, Sun Yat-Sen University, Zhuhai 519082, China

[4]School of Geography, Queen Mary University of London, Bethnal Green, London E1 4NS, United Kingdom

[5]Interface Geochemistry, GFZ German Research Centre for Geosciences, 14473 Potsdam, Germany.

[6]School of Ecosystem and Forest Sciences, University of Melbourne, Richmond, VIC 3121, Australia

[7]School of Chemistry, Monash University, Clayton VIC 3800, Australia

[8]Department of Earth Sciences, University of Southern California, Los Angeles, CA 90089, United States

Correspondence:

* Assoc Prof Chris Greening, Monash University, Department of Microbiology, Innovation Walk, Clayton, VIC 3800, Australia

Email: chris.greening@monash.edu, Ph: +61 451 085 339, ORCID: 0000-0001-7616-0594

* Dr Eleonora Chiri, Monash University, Department of Microbiology, Innovation Walk, Clayton, VIC 3800, Australia

Email: eleonora.chiri@monash.edu, Ph: +61 3 9902 0123, ORCID: 0000-0002-6627-0762

Revised Article Submitted to *Nature Microbiology*

September 2020

Abstract

Soil microorganisms globally are thought to be sustained primarily by organic carbon sources. Certain bacteria also consume inorganic energy sources such as trace gases, but they are presumed to be rare community members, except within some oligotrophic soils. Here we combined metagenomic, biogeochemical, and modelling approaches to determine how soil microbial communities meet energy and carbon needs. Analysis of 40 metagenomes and 757 derived genomes indicated over 70% of soil bacterial taxa encode enzymes to consume inorganic energy sources. Bacteria from 19 phyla encoded enzymes to use the trace gases hydrogen and carbon monoxide as supplemental electron donors for aerobic respiration. In addition, we identified a fourth phylum (Gemmatimonadota) potentially capable of aerobic methanotrophy. Consistent with the metagenomic profiling, communities within soil profiles from diverse habitats rapidly oxidized hydrogen, carbon monoxide, and to a lesser extent methane below atmospheric concentrations. Thermodynamic modelling indicated that the power generated by oxidation of these three gases is sufficient to meet the maintenance needs of the bacterial cells capable of consuming them. Diverse bacteria also encode enzymes to use trace gases as electron donors to support carbon fixation. Altogether, these findings suggest that trace gas oxidation confers a major selective advantage in soil ecosystems, where availability of preferred organic substrates limits microbial growth. The observation that inorganic energy sources may sustain most soil bacteria also has broad implications for understanding atmospheric chemistry and microbial biodiversity in a changing world.

Introduction

Bacteria mediate key supporting and regulatory services in soil ecosystems worldwide [1,2]. Culture-independent surveys have shown that soils harbor abundant and diverse bacterial communities [3,4], with most cells thought to be in dormant states due to pressures such as resource limitation [5,6]. Most soil bacteria use organic carbon derived from vegetation and other inputs as energy and carbon sources [1,7]; reflecting this, isolates from all nine of the most abundant phyla in soils are aerobic organotrophs [8,9]. However, various bacteria have been characterized that use inorganic energy sources, including molecular hydrogen (H_2), carbon monoxide (CO), sulfide, thiosulfate, ammonia, and nitrite [10,11]. While these lithotrophs have key ecological and biogeochemical roles [1,10], they are generally thought to be minor community members compared to organotrophs [1,12].

Emerging evidence suggests the trace gases H_2, CO, and to a lesser extent methane (CH_4) are particularly important energy sources for bacterial growth and survival. These three gases are ubiquitously available in the atmosphere at average global concentrations of 0.53, 0.10, and 1.85 parts per million (ppmv) respectively, with local CO levels varying greatly due to natural and anthropogenic processes [13–16]. These compounds are also produced within soils: H_2 through biological nitrogen fixation and fermentation [13,17,18], CO primarily through abiotic thermal and photochemical processes [15,19], and CH_4 primarily through methanogenesis [16]. Biogeochemically, soil bacteria are major sinks of reduced trace gases, accounting for the net loss of approximately 75% atmospheric H_2 (70 teragrams per year) [13,17], 10% atmospheric CO (250 teragrams per year) [15,20], and 5% CH_4 when excluding wetlands (30 teragrams per year) [16,21]. Microorganisms have evolved specialized metalloenzymes, namely uptake [NiFe]-hydrogenases, [MoCu]-carbon monoxide dehydrogenases, and methane monooxygenases, to oxidize these gases, including below atmospheric concentrations [21–24]. Some bacteria sustain autotrophic or mixotrophic growth by using electrons derived from H_2 and CO to drive aerobic respiration and carbon fixation through various pathways [25–28]. In addition, bacterial cultures from four phyla (Actinobacteriota, Proteobacteria, Acidobacteriota, Chloroflexota) have been shown to switch from growth on organic carbon to persistence on these trace gases in response to carbon starvation [22–24,29,30]. Genetic studies have shown that such metabolic flexibility provides a selective advantage under conditions of low resource availability or stability [18,24,31–33].

Despite these advances, we lack a holistic understanding of the relative contributions of trace gases and other compounds in sustaining the energy and carbon needs of soil communities [34]. Some have hypothesized that trace gas oxidizers may be widespread community members [20,24,26]. However, previous soil surveys reported that atmospheric H_2 and CO oxidizers are

members of the rare biosphere, each comprising just 1% of the total bacterial community, similarly to methane-oxidizing bacteria (methanotrophs) [12,35,36]. Notable exceptions include some extreme environments, such as Antarctic deserts, where trace gas oxidizers are major primary producers in soils with otherwise low photosynthetic input [37–39]. Here, we combined metagenomic, biogeochemical, and thermodynamic modelling approaches to profile metabolic strategies of soil bacteria. We reveal facultative trace gas oxidizers are highly abundant and phylogenetically diverse members of soil microbiomes. Moreover, consumption of trace gases by these bacteria would be sufficient to sustain their basal energy needs.

Results and Discussion

Most soil bacteria harbor the flexibility to oxidize organic and inorganic energy sources

First, we sequenced metagenomes from depth profiles of four Australian soil ecosystems (wetland, grassland, forest, dryland) **(Supplementary Tables 1 & 2)** and analyzed metagenomes from eight further global sites **(Supplementary Table 2)**. Assembly and binning yielded 757 high- or medium-quality metagenome-assembled genomes (MAGs) spanning 26 bacterial and five archaeal phyla **(Supplementary Table 3)**. Consistent with the community composition of the sites **(Extended Data Fig. 1; Supplementary Table 4)**, half of the genomes affiliate with globally dominant soil phyla [3,8] Actinobacteriota, Proteobacteria, and Acidobacteriota.

We used comprehensive reference databases **(Supplementary Table 5)** to search key metabolic genes in metagenomic short reads and derived genomes **(Fig. 1; Supplementary Tables 6 & 7)**. As anticipated [1], most bacteria have the capability to conserve energy through aerobic respiration of organic compounds. More surprisingly, many of these bacteria also encoded the key enzymes (group 1 and 2 [NiFe]-hydrogenases and form I CO dehydrogenases) to consume trace gases H_2 and CO: an average of 39% and 56% of the bacterial community based on short reads, and 31% and 26% of assembled genomes. Also widespread was the capacity for sulfide (28% community / 22% genomes) and thiosulfate (6.2% / 11%) oxidation, whereas nitrite (4.6% / 3.7%), ammonium (1.5% / 2.4%), and methane (1.1% / 0.37%) oxidation and photosynthesis (1.3% / 1.5%) were more restricted traits **(Fig. 1)**. Altogether, on average 72% of bacterial genomes encoded enzymes to acquire energy *via* inorganic substrates. For electron acceptor utilization, most bacteria encoded terminal oxidases for aerobic respiration and many were predicted to conserve energy by nitrate reduction (25% / 14%), nitrite reduction (21% / 21%), and hydrogenogenic fermentation (29% / 21%) **(Fig. 1)**. Consistent with these results, for three global sites with accompanying metatranscriptome data **(Supplementary Table 2)**, read mapping confirmed the most expressed respiratory genes encoded terminal oxidases (av. 594 transcripts per million, TPM) and enzymes for oxidation of NADH (198 TPM), H_2 (126 TPM), CO (75 TPM), and ammonium (223 TPM) **(Extended Data Fig. 2; Supplementary Table 8)**. Altogether, these observations suggest that a large proportion of soil bacteria are metabolically flexible organoheterotrophs, which encode and express enzymes to use alternative energy sources such as trace gases to supplement energy needs.

Diverse bacterial phyla are capable of oxidizing H_2, CO, and CH_4 in different soil ecosystems

To gain insight into phylogenetic diversity of trace gas oxidizers, we generated phylogenetic trees of the uptake hydrogenases and CO dehydrogenases from binned and unbinned assembled sequences **(Supplementary Table 9)**. 19 phyla encoded one or both enzymes, including all nine dominant soil phyla (Acidobacteriota, Actinobacteriota, Bacteroidota, Chloroflexota, Firmicutes, Gemmatimonadota, Planctomycetota, Proteobacteria, Verrucomicrobiota) [3,8] and six candidate phyla (Binatota, Dormibacterota, Eremiobacterota, Methylomirabilota, Tectomicrobia, UBP7). Among the uptake hydrogenases, 49% of the 1522 hits affiliated with group 1h [NiFe]-hydrogenases. This relatively recently discovered high-affinity enzyme supports persistence of organotrophic bacteria by oxidizing atmospheric H_2 [22,23,26,30,40,41]. The phylogenetic tree revealed an unprecedented sequence diversity and broad taxonomic distribution of this subgroup, with sequences affiliated with 13 phyla **(Fig. 2a; Supplementary Fig. 1)**. Also widespread were various radiations within the group 1d (8.9%), 1f (19%), and 2a (3.6%) [NiFe]-hydrogenases known to support aerobic hydrogen oxidation [23,26,28,42,43], as well as a subclade of the group 1c hydrogenases (13%) encoded by Acidobacteriota, Planctomycetota, and Gemmatimonadota **(Fig. 2a; Supplementary Figs. 2 & 3)**. For CO dehydrogenases, we restricted our searches to the canonical form I enzyme using recently described reference databases [24], given there is no strong evidence that CO is the physiological substrate of the related form II enzyme [20,24,29,44]. The form I CO dehydrogenase was similarly prevalent across the MAGs; the tree shows large actinobacterial and proteobacterial clades flanking a central mixed clade containing sequences from 11 different phyla **(Fig. 2b; Supplementary Fig. 4)**. In line with previous inferences [24,26], both trees suggest enzymes for trace gas oxidation were horizontally disseminated between bacteria on multiple occasions.

Phylogenetic analysis also validated the presence and affiliations of sulfide, thiosulfate, ammonia, nitrite, and methane oxidizers **(Supplementary Figs. 5 to 10; Extended Data Fig. 3)**. These included genomes of soil comammox bacteria [45,46] and a potential nitrite-oxidizing bacterium within recently reported candidate phylum Eremiobacterota [37]. A major finding was the recovery of a high-quality Gemmatimonadota bin predicted to use methane, hydrogen, and acetate as energy sources. Its genome encodes a putative particulate methane monooxygenase that forms a sister lineage to those of the recently discovered *Candidatus* Methylomirabilota methanotrophs (sharing ~60% sequence identity) and corresponds to amplicon sequences previously identified for the ubiquitous uncultivated putative methanotroph lineage TUSC

(Tropical Upland Soil Cluster) [47,48]. Protein modelling suggests that this enzyme shares a common tertiary structure and copper-binding residues with canonical particulate methane monooxygenases **(Extended Data Fig. 3)**. Altogether, these results suggest that Gemmatimonadota is a fourth phylum [49–51] capable of aerobic methanotrophy, though cultivation and biogeochemical studies are required to confirm its activity. We propose this bacterium is named *Candidatus* Methylotropicum kingii **(Etymological Information)**.

Trace gas oxidizers are highly active across different soil habitats and depths

Reflecting their abundance and diversity, we confirmed that trace gas oxidizers are active in soil communities of all investigated Australian soils. *In situ* concentrations and soil-atmosphere fluxes of H_2, CO, and CH_4 were measured across the four sites in biological quadruplicate using a sensitive gas chromatograph **(Supplementary Table 10)**. All three gases were present within typical mixing ratios [13,15,16] at the soil-atmosphere interface and top 20 cm of each soil **(Fig. 3a)**, confirming these substrates are available to bacteria. Gas concentrations decreased with depth at some sites **(Extended Data Fig. 4)**, potentially indicating microbial consumption. There was also potential evidence of endogenous gas production within some soil profiles: the elevated H_2 concentrations in deeper wetland soils may result from activity of the numerous hydrogenogenic fermenters (33% community / 32% genomes; **Extended Data Fig. 5**) under hypoxic conditions [18], whereas the elevated gas levels in the dryland soils are consistent with photochemical and thermal production processes [52]. In turn, endogenous production would result in some cryptic gas cycling within the soil profile, though this remains to be experimentally verified. In line with the abundance of H_2 oxidizers, net *in situ* H_2 uptake was observed by soil communities at all sites and consumption was particularly rapid at the grassland, forest, and wetland sites **(Fig. 3b)**; ambient H_2 in the flux chambers was oxidized by underlying soil down to a threshold of ~0.1 ppmv within a few minutes, resulting in typical fluxes of -10 to -40 nmol m^{-2} s^{-1}. In contrast, no significant fluxes of CO were observed; the high rates of photochemical CO production known to occur during daylight potentially obscured underlying microbial consumption [19,53], though this remains to be experimentally confirmed. Reflecting global patterns [54], with the exception of forest sites, CH_4 uptake fluxes were low in comparison with H_2. Control experiments confirmed the flux chambers were gas-tight and did not mediate significant gas production or consumption during the timecourse of the flux measurements **(Extended Data Fig. 4)**. Overall, the trace gas fluxes observed are much lower than typically reported for heterotrophic respiration [7], although endogenous soil production potentially obscures much consumption.

We subsequently measured *ex situ* oxidation rates by incubating samples from soil depth profiles in serum vials containing ambient air headspaces **(Supplementary Table 10)**. Under these conditions, biological gas consumption could be accurately quantified given no significant abiotic production of these gases was detected **(Extended Data Fig. 6)**. Atmospheric H_2 and CO were both rapidly oxidized by forest, grassland, and wetland soils at rates within fivefold of previous literature [10,55–58]. Bulk rates were significantly higher for topsoils (0-5 and 5-10 cm) compared to deeper soils (15-20 and 25-30 cm) **(Supplementary Table 10; Extended Data Fig. 6)**, though cell-specific rates (normalized to estimated number of respective trace gas oxidizing cells; **Extended Data Fig. 7**) showed few significant variations with depth **(Fig. 3c; Supplementary Table 11)**. Across these sites, atmospheric CH_4 oxidation occurred at 76-fold and 35-fold lower rates than H_2 and CO on average, with the most rapid consumption again occurring at the forest site. Such observations are consistent with the much higher levels of uptake hydrogenases and CO dehydrogenases compared to methane monooxygenases in the metagenomes and derived genomes **(Fig. 1)**. In line with the *in situ* observations, trace gas oxidation was slowest for dryland soils. This possibly reflects that, as observed in previous laboratory studies, low water content inhibits trace gas uptake [44,45]. Contrary to the pattern observed in other habitats, deeper dryland soils consumed trace gases more rapidly, perhaps reflecting their higher measured water content **(Supplementary Table 1)**. Experimentally wetting dryland soils, in order to simulate rainfall events, enhanced rates by an average of 60-fold **(Fig. 3c; Extended Data Fig. 6)**. Together, these activity-based measurements complement the metagenomic analysis by confirming soil communities contain highly active H_2, CO, and sometimes CH_4 oxidizers. While net *in situ* gas fluxes were often low or variable, especially for CO, the rapid *ex situ* rates and previous reports of endogenous gas production [18,19,52,53,59] suggest high levels of internal gas cycling likely occurs.

Trace gases enable persistence of most soil bacteria and may support mixotrophic growth

Trace gas oxidation is likely to primarily support the persistence of organotrophic bacteria. Most sequenced soil bacteria encoded uptake hydrogenases and CO dehydrogenases together with the genes for organotrophy. Based on observations from pure culture studies, bacteria consume trace gases to conserve energy for cellular maintenance when organic carbon supplies are limiting for growth [3–5,30]. We used thermodynamic modelling to predict the amount of power (i.e. energy per time in J s^{-1} (W)) per cell **(Supplementary Table 12)** that could be generated based on the *ex situ* oxidation rates **(Extended Data Fig. 6)** and the total number of putative trace gas oxidizers detected per gram of dry soil **(Fig. 1 & Extended Data Fig. 7)**.

Oxidation rates were sufficient to generate an average power of 2.2×10^{-15} W per H_2-oxidizing cell, 2.0×10^{-15} W per CO-oxidizing cell, and 1.1×10^{-13} W per CH_4-oxidizing cell, and trends were similar across habitats and depths with the exception of the dryland soils **(Fig. 3d & Supplementary Table 12)**. The calculated cell-specific power values are within the broad range of the maintenance and endogenous energy requirements previously reported for various laboratory-grown cultures of aerobic heterotrophs (average 1.9×10^{-15} W per cell [60]; range 10^{-12} to 10^{-17} W per cell [60–63]) and greatly exceed the *in situ* maintenance energies of aerobic heterotrophs in highly energy-limited ecosystems (10^{-17} to 10^{-19} W per cell [64–66]). Previous studies estimated the theoretical maximum population of trace gas oxidizers based on observed oxidation rates and the assumption of a single static maintenance energy [67–69]. Although our experimentally observed population is in reasonable agreement with such estimates, results are sensitive to the assumed maintenance energy **(Extended Data Fig. 8)**. Literature data and our cell-specific power calculations based on empirical parameters suggest that metabolic rates are highly variable between microbial populations, metabolic strategies, and soil habitat. Therefore, the use of a single maintenance energy to estimate the fraction of the population that can be supported by trace gas oxidation may be too simplistic. It should also be noted that our estimates did not account for relic DNA [70], inactive cells, and cryptic gas cycling. Thus, gross oxidation rates and available power per active cell may be considerably higher *in situ*. Altogether, this suggests that trace gases alone can theoretically sustain the persistence of the entire gas-consuming community.

Trace gases may also support mixotrophic growth of a significant proportion of bacteria across these soil habitats. Our analysis indicates that most community members, including trace gas oxidizers, acquire carbon heterotrophically. However, some bacteria (13% community / 12% genomes) encoded the capacity to assimilate CO_2 through the Calvin-Benson cycle **(Fig. 1)**. Genome-resolved analysis indicated most of these autotrophs were capable of oxidizing H_2 (79%) and/or CO (63%), with some predicted to mediate sulfide oxidation (32%), thiosulfate oxidation (17%), or photosynthesis (11%) **(Supplementary Table 7)**. Putative autotrophic H_2 and CO oxidizers were patchily distributed among seven dominant soil phyla and candidate phylum Dormibacterota, suggesting autotrophy has been acquired multiple times **(Fig. 1)**. Consistently, phylogenetic analysis showed that the 93% of the binned ribulose 1,5-bisphosphate carboxylase / oxygenase (RuBisCO / RbcL) hits were from clades known to support chemosynthesis rather than photosynthesis **(Extended Data Fig. 9)**. Reads for other CO_2 fixation pathways were also detected, but with exception of the peatland sample, were encoded by less than 1% of the total community **(Fig. 1; Supplementary Table 6)**. Individual atmospheric trace gases are thought to be insufficiently concentrated to sustain growth as the sole energy source

[10,67], though there is increasing evidence that they can sustain mixotrophic growth [27,28,71]. Moreover, autotrophic growth may be favorable in environments where there are significant rates of edaphic gas production, for example due to hydrogenogenic fermentation **(Extended Data Fig. 5)** during hypoxia [28]. Remarkably, this suggests that the process of atmospheric chemosynthesis recently discovered in Antarctic deserts [9] extends to other habitats.

Conclusions and Outlook

Overall, bacteria with the metabolic flexibility to use both organic and inorganic energy sources are likely to have a selective advantage in soil environments. In most soils, organic carbon is the main factor limiting microbial growth [13,49]; this reflects the inherent spatiotemporal variability in organic carbon availability of soils, together with the recalcitrance of many organic polymers and the intense competition for more degradable compounds [1]. Thus, the ability to consume alternative energy sources is likely to be critical for adaptation and resilience of many taxa. H_2 and CO are ideal compounds in this regard given they are readily available from both atmospheric and edaphic sources; likewise, their high energy content, low activation energy, and diffusibility into microbial cells make these gases dependable for persistence [31,50].

Our findings in turn suggest that oxidation of these trace gases is a generalist process, rather than a specialist one as previously suggested [6]. We provide multiple lines of evidence that H_2 and CO oxidizers are abundant, diverse, and active across different soil habitats and depths. These findings strikingly contrast with some previous reports that trace gas oxidizers comprise just 1% of the community [12,35]. Such discrepancies might reflect that previous work on atmospheric H_2 oxidizers relied on non-degenerate quantitative PCR primers that only capture a small proportion of the total diversity of soil uptake hydrogenases; indeed, we observed high proportions of high-affinity hydrogenases (30% community / 40% genomes) in the Canadian cropland metagenome where H_2 oxidizers were previously inferred to be minor community members [6,7]. Moreover, while previous genome surveys indicate Actinobacteriota predominantly mediate atmospheric H_2 oxidation [33,37], our analysis indicates all major bacterial soil phyla can mediate this process. However, an important caveat is that our findings are based primarily on genomic inferences and bulk rates, meaning it is unclear if all putative trace gas oxidizers were active during the experiments. Such metabolically flexible generalists co-exist with more specialist taxa that are predicted to use more niche substrates, including methane, ammonia, and nitrite. The finding that some Gemmatimonadota encode genes for aerobic methane oxidation further indicates the diversity of trace gas oxidizers in soils. Our results also reveal an

unexpected diversity and abundance of chemoautotrophs in soils, while hinting at roles for sulfur-based compounds as further supplementary energy sources.

The thermodynamic calculations suggest that trace gas oxidation is sufficient to sustain the persistence of all trace gas oxidizers and thus most bacteria in soils. Power per cell values are well within the range of maintenance or endogenous energies typically reported for pure cultures, and exceed the range for energy-limited ecosystems [60–64]. Nevertheless, there is likely to be considerable heterogeneity in the rates that individual cells oxidize trace gases and the way they allocate energy derived from this process. For example, it is plausible that whereas some cells encoding uptake hydrogenases minimally use H_2, many others will depend on this gas for survival and yet others may use it to support growth. It is also critical to note that most bacteria harboring genes for trace gas oxidation are predicted to be metabolically flexible. Many of them are likely to simultaneously consume organic and inorganic energy sources, or indeed several trace gases together as recently inferred for a methanotroph predicted to grow on atmospheric energy sources alone [27], in order to grow or persist mixotrophically. Innovative studies are required to gain a detailed perspective on how trace gases are differentially used within and between bacterial populations and cells.

More broadly, the extensive soil-atmosphere interaction described here appears to be a key regulator of soil biodiversity and atmospheric chemistry. As summarized in **Extended Data Fig. 10**, soil bacteria consume trace gases of atmospheric, biological, and geochemical origin. Given trace gases are major energy sources sustaining the dormant soil majority, their oxidation will in turn influence wider community ecology; indeed, it is well-established that dormancy contributes to the maintenance of microbial biodiversity and the resilience of soil communities [17]. Moreover, the observation that trace gas oxidizers are more numerous and diverse than previously thought suggests the global atmospheric sinks of H_2 and CO are relatively resilient. This may explain why, despite high anthropogenic emissions of H_2, global mixing ratios have remained quite stable [26]. Nevertheless, various human activities could undermine this soil-atmosphere interaction, for example through changing soil properties (e.g. through agricultural practices and desertification) and atmospheric composition (e.g. through urban pollution or a hydrogen economy [51]), with potential ecological and biogeochemical ramifications. Further studies are required to understand what physicochemical factors influence the abundance and activities of trace gas oxidizers, and how they respond to local and global change. More work is also needed to understand the role of chemosynthetic CO_2 fixation by soil trace gas oxidizers, which appear to include the most abundant bacterial autotrophs in aerated soils, and in turn determine whether this process serves as a significant CO_2 sink.

Methods

Site description and sampling. Sampling was conducted in four sites within Australia: (i) wetland (-37.908647°, 145.139591°; Jock Marshall Reserve, Clayton, VIC; JMR), (ii) forest (-37.446379°, 144.470078°; Wombat State Forest, VIC; WSF), (iii) grassland (-37.926514°, 145.313136°; Don Bosco Grassland, Lysterfield, VIC; DBG), and (iv) dryland (-23.977765°, 133.712524°; 25.5 km south of Alice Springs, NT; ASD). The sites were sampled on December 19 2018, January 5 2019, January 21 2019, and January 29 2019 respectively. At each site (~100 m^2), four sampling plots (~1 m^2) were selected. At each plot, *in situ* depth-resolved gas concentrations profiles and soil-atmosphere fluxes were measured. In addition, a core was used to collect soil samples at four depths (0-5, 5-10, 15-20, and 25-30 cm) for *ex situ* oxidation measurements, physicochemical analysis, and DNA extractions to perform quantitative polymerase chain reactions (qPCR) and metagenomic sequencing. All sampling occurred during daylight hours and dry weather conditions, gas samples were processed within 48 h of collection, and soil samples were incubated for *ex situ* oxidation measurements within 24 h of collection.

Sampling and measurement of soil gas profiles. Depth-resolved *in situ* gas concentrations of H_2, CO, and CH_4 were measured using stainless steel capillaries of 1 mm internal diameter fitted with a Luer Lock and Discofix three-way stopcock. Prior to sampling, each capillary was inserted into the soil at depth intervals of 2, 4, 6, 8, 10, and 16 cm. All capillaries were installed simultaneously, arranged in a hexagonal grid (diameter ~20 cm), and left to equilibrate for ~30 min. Samples of 15 mL were withdrawn using a 20 mL gas-tight Terumo syringe. A gas sample was also collected at the soil-atmosphere interface (0 cm). All gas samples were stored in evacuated 12 mL glass exetainers sealed with rubber septum lids and analyzed using gas chromatography. Gas concentrations in samples were measured by gas chromatography using a pulsed discharge helium ionization detector (model TGA-6791-W-4U-2, Valco Instruments Company Inc.) as previously described [72]. Samples were calibrated against H_2, CO and CH_4 standards that were prepared using ultra-pure concentrations of each gas (1% in N_2 gas cylinder, 99.999% pure, Air Liquide Australia) down to the limit of quantification (H_2 20 ppbv, CO 90 ppbv, CH_4 500 ppbv. Pressurized air (Air Liquide Australia) with known trace gas concentrations was used as an internal reference standard.

Measurement of soil-atmosphere gas fluxes. *In situ* soil-atmosphere fluxes of H_2, CO, and CH_4 were measured using static flux chambers. The chamber consisted of a polyvinylchloride (PVC) pipe of 20 cm height and 15 cm diameter with a threaded access cap. The cap was fitted with a

gastight O-ring, two butyl rubber septa (one for air sampling and one for a thermometer), and an axial fan on the inside to promote internal mixing. At each plot, a PVC base collar of 10 cm height and 14.8 cm diameter was inserted ~5 cm into the soil and left to equilibrate for ~30 minutes prior to sampling to reduce lateral gas fluxes. Once the chamber was fitted over the collar, the cap was closed and the axial fan was started. Three consecutive gas measurements were taken at approximately one-minute intervals, followed by either four or five measurements at approximately five-minute intervals. For each measurement, 15 mL of gas was collected using a gas-tight 20 mL Terumo syringe fitted with a Luer Lock and Discofix three-way stopcock and measured by gas chromatography as described above. Control gas measurements of ambient air were taken directly before, during, and after sampling. The temperature of the chamber, ambient air, and soil were monitored throughout. Concentrations were then converted to nmol m^{-3} at ambient pressure and temperature using the ideal gas law. Atmospheric flux (J_{atm}) was calculated from the concentration (C_0) and rate change (dC/dt) at chamber deployment using a linear regression (eq. 1) and an exponential model fit (eq. 2 and eq. 3) [59] for each chamber measurement:

$$J_{atm} = h\frac{dC}{dt} \quad \text{(EQ. 1)}$$

$$C_{(t)} = \frac{P}{k} + \left(C_0 - \frac{P}{k}\right)e^{(-kt)} \quad \text{(EQ. 2)}$$

$$J_{atm} = h(P - kC_0) \quad \text{(EQ. 3)}$$

For the exponential model, parameters P and k were fitted via non-linear regression using the nls() function in R. h denotes the effective chamber height in m. The best model was chosen according to the lower Akaike information criterion (AIC). Conservative flux detection limits incorporating errors of sample handling and storage were calculated using mean and standard deviation of air samples [73]. Three independent incubations were conducted to control for trace gases potentially leaked from the chamber or released in the chamber headspace by plastic components due to abiotic processes. Chambers were placed on an inert stainless steel surface and sealed on the surface with silicone grease. Headspace samples from eight time points and three air samples were collected following measurement setup, incubation time, and sampling procedures described above for the *in situ* sampling of actual samples. No variation in trace gas concentration was observed during the incubation time **(Extended Data Fig. 8)**.

Soil sampling and physicochemical analysis. Four soil cores of 30 cm depth were collected from each site (16 total). Cores were carefully extracted and immediately segmented at 5 cm depth intervals before being transferred into 50 mL Falcon tubes. At four different depth intervals (0-5, 5-10, 15-20, 25-30 cm), a subset of 10 g of soil was frozen at -20°C for community DNA extraction and a subset of 5 g was used within 24 hours for gas chromatography studies. Additional surface soil was collected using a 10 × 5 cm bulk density ring to estimate bulk density and soil water content, which was measured gravimetrically using a drying oven at 140°C. For soil chemistry analysis, surface soil samples (0-5 cm) from each plot were pooled to form one representative composite sample per site and sent to the Environmental Analysis Laboratory (EAL), Southern Cross University. In total, 21 separate soil chemical parameters were selected for analysis, based on commonly reported drivers of soil microbial composition globally. These included: soil acidity (pH), electrical conductivity (EC), effective cation exchange capacity (ECEC), total organic carbon, total nitrogen, sodium (Na), sulfur (S), phosphate (P), potassium (K), nitrate (NO_3^-), and ammonium (NH_4^+), as well as bioavailable manganese (Mn), copper (Cu), zinc (Zn), boron (B), aluminium (Al), iron (Fe), and silicon (Si). In addition, particle size analysis by hydrometry was performed to estimate the percentage of gravel, sand, silt, loam, and clay **(Supplementary Table 1)**.

***Ex situ* oxidation rates**. To determine the capacity of the soils to oxidise trace gases at atmospheric concentrations, 5 g soil from the four depth intervals (0-5, 5-10, 15-20, 25-30 cm) were placed in 120 mL serum vials. The headspace was repeatedly flushed with air from a pressurized cylinder (Air Liquide, Australia) to achieve headspace mixing ratios reflecting atmospheric levels (~0.5 ppmv H_2, ~0.6 ppmv CO, ~1.8 ppmv CH_4). Sampling commenced immediately after sealing the vial and headspace samples of 2 mL were taken at 10 min intervals for 40 minutes. While this timecourse sufficiently captured oxidation rates for most samples, additional gas samples were collected every 24 hrs for up to nine days to capture oxidation rates of soils that mediated slow gas consumption. Gas concentrations were measured by gas chromatography as described above. Heat killed soils (two 30-minute autoclave cycles at 121°C) and blank measurements (empty serum vials) were used as controls, confirming trace gas oxidation from samples occurred due to biotic processes. Given the low capacity of dryland soils to oxidize atmospheric trace gases, we simulated soil wetting conditions due to a rainfall event to determine whether soil hydration enhances activity. To do this, we used a custom Perspex collar fitted with a water-draining stainless steel woven mesh (0.17 mm) and a water-catching tray. Collars were sterilised using ethanol and soils (5 g) were placed in the centre of the mesh surface. Soils were watered until fully saturated by repeated addition of MilliQ water. Once fully

saturated, each collar was sealed at the top using clingfilm to avoid evaporation and left to drain for 24 hrs in the dark. Once drained, soil samples were transferred using sterile techniques into a 120 mL serum vial and gas oxidation was measured as described in the previous section. Similar to *in situ* fluxes above, reaction rates were calculated from the first five data points using first- and zero-order reaction models, with the best rate chosen according to AIC. The data was tested for normality using a Shapiro-Wilk test. To test for significant difference in oxidation rates between ecosystems and depths, a non-parametric one-way Kruskal-Wallis test was used. This was followed by a pairwise Wilcox Rank Sum test to test significant relationships between pairs. *p* values were adjusted using a Benjamini Hochberg correction.

Community DNA extraction. At each soil depth sampled per site, soils from the four plots were pooled together. For each of the 16 resultant samples, total community DNA was extracted using 0.25 g soil. Extractions were performed using the MoBio PowerSoil Isolation kit according to the manufacturer's instructions. Samples were eluted in DNase- and RNase-free UltraPure Water (ThermoFisher). A sample-free negative control was also run. Nucleic acid purity and yield were measured using a NanoDrop ND-1000 spectrophotometer and a Qubit Fluorometer 2.0.

Quantitative PCR. Quantitative polymerase chain reactions (qPCR) were used to estimate total bacterial and archaeal biomass. The 16S rRNA gene was amplified using the degenerate primer pairs 515F (GTGYCAGCMGCCGCGGTAA) and 806R (GGACTACNVGGGTWTCTAAT) [74]. A synthetic *E. coli* 16S rRNA gene sequence in a pUC-like cloning vector (pMA plasmid; GeneArt, ThermoFisher Scientific) was used as a standard. PCR reactions were set up in each well of a 96-well plate using a LightCycler 480 SYBR Green I Master Mix. Each sample was run in triplicate and standards in duplicate on a LightCycler 480 Instrument II (Roche). The qPCR conditions were as follows: pre-incubation at 95°C for 3 min and 45 cycles of denaturation 95°C for 30 s, annealing at 54°C for 30 s, and extension at 72°C for 24 s. 16S rRNA gene copy numbers were calculated based on a standard curve constructed by plotting average Cp values of a serial dilution of the plasmid-borne standard against their copy numbers.

Sequencing, assembly, and binning of Australian metagenomes. Metagenomic shotgun libraries were prepared for the 16 samples using the Nextera XT DNA Sample Preparation Kit (Illumina Inc., San Diego, CA, USA). Sequencing was performed on an Illumina NextSeq500 platform with a 2 × 150 bp High Output run. Raw reads derived from the 16 metagenome libraries were quality-controlled by clipping off primers and adapters then filtering out artifacts and low-quality reads using Read_QC module within the metaWRAP pipeline [75]. For each

ecosystem, the four quality-controlled metagenomes were co-assembled using MEGAHIT v1.1.3 [76] (default parameters) and individually assembled using SPAdes v3.13.0 [77] (metaSPAdes mode, default parameters), producing five assemblies for each ecosystem. Short contigs (<1000 bp) were removed. Each assembly was binned using the binning module within the metaWRAP [75] pipeline (MetaBAT [78], MetaBAT2 [79], and MaxBin2 [80]). For each assembly, the three bin sets were then consolidated into a final bin set with the bin_refinement module of metaWRAP [75]. For each ecosystem, the final bin sets were aggregated and de-replicated using dRep [81] (-comp 50 -con 10 options). Completeness, contamination, and heterogeneity of each bin were estimated using CheckM [82], with medium- and high-quality bins (completeness >50%, contamination <10%) [83] retained for further analysis. After dereplication, a total of 93 metagenome-assembled genomes (MAGs) were obtained for the four ecosystems. Each bin was taxonomically assigned according to the Genome Taxonomy Database (GTDB; release 04-RS89) [84] using GTDB-tk [85].

Assembly and binning of global public soil metagenomes. A total of 24 previously sequenced metagenomes from eight different soil ecosystems (three metagenomes for each ecosystem) **(Supplementary Table 2)** were downloaded from the Integrated Microbial Genomes database [86] and the NCBI Sequence Read Archive (SRA) [87]. These comprised: Barrow Environmental Observatory site, Barrow, Alaska, USA (Arctic Tundra, BEO) [88]; St. Claude, Quebec, Canada (Agricultural Land – Crop Rotation, SCQ) [89]; Kellogg Biological Station, Michigan, USA (Agricultural Land – Switchgrass, KBS) [90]; Algoma, Ontario, Canada (Coniferous Forest, ALO) [91]; Anza Borrego Desert, California, USA (Hot Desert, ABD) [92]; Department of Meta, Colombia (Tropical Peatland, DMC) [93]; National Park of Serra do Cipo, Brazil (Rupestrian Grassland, NPS) [94]; and Luquillo Experimental Forest, Rio Grande, Puerto Rico (Tropical Rainforest, LEF) [95]. Raw reads derived from the 24 metagenome libraries were quality-controlled by clipping off primers and adapters and filtering out artefacts and low-quality reads using Read_QC module in the metaWRAP pipeline [75]. For each ecosystem, the three quality-controlled metagenomes were both co-assembled and individually assembled using MEGAHIT v1.1.3 [76], producing four assemblies for each ecosystem. For the assembly process, all of them used default parameters except co-assembly of metagenomes for Kellogg Biological Station (--k-min 27). Short contigs (<1000 bp) were removed. Each assembly was binned using the binning module within the metaWRAP [75] options (MetaBAT [78], MetaBAT2 [79] and MaxBin2 [80]) except assemblies derived from Kellogg Biological Station and Luquillo Experimental Forest where only MetaBAT2 [79] was used. Dereplication and quality-control of produced bins were performed as above. After dereplication, a total of 664 high- or medium-quality MAGs were obtained for the eight ecosystems. Each bin was taxonomically assigned as above.

Functional annotation of binned and unbinned contigs. The sequences of 43 marker genes representing energy conservation and carbon acquisition processes were retrieved from binned and unbinned contigs. Open reading frames (ORFs) were first predicted using Prodigal v.2.6.3 [96] and genes were annotated using a combination of homology-based searches and hidden Markov model (HMM) searches. For homology-based searches, predicted ORFs were searched using DIAMOND *blastp* [97] against 32 custom protein databases described below. These encompassed the genes encoding ATP-citrate lyase (AclB), acetyl-CoA synthase (AcsB), ammonia monooxygenase (AmoA), anaerobic sulfite reductase (AsrA), anaerobic carbon monoxide dehydrogenase (CooS), form I aerobic carbon monoxide dehydrogenase (CoxL), dissimilatory sulfite reductase (DsrA), flavocytochrome *c* sulfide dehydrogenase (FCC), 4-hydroxybutyryl-CoA synthase of Crenarchaeota (HbsC), 4-hydroxybutyryl-CoA synthase of Thaumarchaeota (HbsT), hydrazine synthase (HzsA), malonyl-CoA reductase of Chloroflexota (Mcr), methyl/alkyl-CoM reductase (McrA), soluble methane monooxygenase (MmoX), periplasmic nitrate reductase (NapA), dissimilatory nitrate reductase (NarG), nitrogenase (NifH), copper-containing nitrite reductase (NirK), cytochrome cd_1 nitrite reductase (NirS), nitrous oxide reductase (NosZ), ammonia-forming nitrite reductase (NrfA), nitrite oxidoreductase (NxrA), particulate methane monooxygenase (PmoA), ribulose 1,5-bisphosphate carboxylase/oxygenase (RbcL), succinate dehydrogenase / fumarate reductase (SdhA / FrdA), sulfur oxygenase/reductase (Sor), thiosulfohydrolase (SoxB), sulfide-quinone oxidoreductase (Sqr), and three hydrogenase classes (NiFe-hydrogenase large subunit, FeFe-hydrogenase catalytic domain, Fe-hydrogenase). DIAMOND mapping was performed with a query coverage threshold of 80% for all databases, and a percentage identity threshold of 60% (AmoA, PmoA, MmoX, CoxL, HbsT, NxrA, RbcL) or 50% (all other databases) and e-value thresholds of 10^{-20}. HMM searches were performed against Pfam and Tigrfam databases using the *annotate* function of EnrichM v.0.5.0 (https://github.com/geronimp/enrichM), with domain noise-cut-off scores as previously described [98]. Eleven genes encoding subunits of ATP synthase (AtpA), two NADH dehydrogenases (NuoF, NqrF), four terminal oxidases (CcoN, CoxA, CydA, CyoA), two photosystems (PsaA, PsbA), formate dehydrogenase (FdhA), and reductive dehalogenase (RdhA) were searched.

Metabolic annotation of metagenomic short reads. For the functional annotation of short reads, paired-end reads in each sample were stripped of adapter and barcode sequences, then contaminating PhiX and low quality sequences were removed (minimum quality score 20) using the BBDuk function of BBTools v. 36.92 (https://sourceforge.net/projects/bbmap/). Resultant

quality-filtered forward reads with lengths of at least 100 bp were searched for the presence of the 43 metabolic marker genes described above using DIAMOND *blastx* algorithm [99]. Specifically, reads were searched against the 32 custom-made reference databases and hits from the 11 HMM searches, using a query coverage of 80% and an identity threshold of either 60% (AmoA, PmoA, MmoX, CoxL, HbsT, NxrA, RbcL) or 50% (all other databases) and a maximum e-value threshold of 10^{-10}. Read counts were normalized to reads per kilobase per million (RPKM) and further normalized against a mean RPKM value estimated from 14 single copy ribosomal marker genes to infer the percentage of the community encoding the gene.

Metabolic annotation of metatranscriptomic reads. Three previously sequenced soil metatranscriptomes collected from sampling locations matching three metagenomes (Extended Data Table S2) were downloaded from the Integrated Microbial Genomes database [16] and the NCBI Sequence Read Archive (SRA) [17]. These comprised: Kellogg Biological Station, Michigan, USA (Agricultural Land – Switchgrass, KBS) [90]; Anza Borrego Desert, California, USA (Hot Desert, ABD) [92]; Department of Meta, Colombia (Tropical Peatland, DMC) [93]. Raw metatranscriptomes were quality filtered as described above and SortMeRNA (version 4.2.0) [100] was used to remove ribosomal RNA (rRNA) reads. To determine transcript abundances of 43 metabolic marker genes described above, filtered reads with lengths of at least 100 bp were searched for their presence using DIAMOND *blastx* and read counts were normalized to reads per kilobase per million (RPKM). To calculate transcript abundances of genes annotated from metagenomic assemblies and MAGs, Salmon v1.3.0 [101] was used in mapping-based mode (salmon quant, --validate Mappings) and read counts were normalised to transcripts per million (TPM). For genes predicted from metagenomic assemblies, they were firstly clustered at 95% sequence identity to produce a non-redundant gene catalog as a 'reference transcriptome' using CD-HIT v4.8.1 [102] before Salmon quantifications.

Phylogenetic analysis. Phylogenetic trees were constructed to understand the distribution and diversity of bacteria and archaea consuming inorganic energy sources. Trees were constructed for the group 1 and 2 [NiFe]-hydrogenase large subunits, group 3 [NiFe]-hydrogenase large subunits, CoxL, PmoA, RbcL, AmoA, NxrA, Sqr, SoxB, and DsrA. In all cases, protein sequences retrieved from the MAGs reads by homology-based searches were aligned against a subset of reference sequences from the custom protein databases using ClustalW in MEGA7 [103]. Evolutionary relationships were visualized by constructing a maximum-likelihood phylogenetic tree; specifically, initial trees for the heuristic search were obtained automatically by applying Neighbour-Join and BioNJ algorithms to a matrix of pairwise distances estimated using a JTT

model, and then selecting the topology with superior log likelihood value. All residues were used and trees were bootstrapped with 50 replicates. To further visualize the diversity of trace gas oxidizers, neighbor-joining trees were constructed using the binned and unbinned sequences for group 1 and 2 [NiFe]-hydrogenase large subunits and CoxL; these trees were constructed using the Poisson model with gaps treated with pairwise deletion and bootstrapped with 50 replicates.

Protein homology modelling. Structural homology models for particulate methane monooxygenase subunits PmoA, PmoB, and PmoC from *Candidatus* Methylotropicum kingii, *Methylacidiphilum infernorum* (PmoA: WP_012463843, PmoB: WP_012463845, PmoC: WP_012463844) and *Candidatus* Methylomirabilis limnetica (PmoA: WP_107560874, PmoB: WP_107560875, PmoC: WP_107560873) were generated using the Phyre2 webserver [104]. Direct threading of Pmo subunit amino acid sequences was performed using the closest structurally characterized particulate methane monooxygenase homologue to each strain, namely those of *Methylocystis* sp. strain M (PDB ID: 3RFR) [105] for *Ca.* M. kingii and *Methylococcus capsulatus* (PDB ID: 3RGB) [105] for *M. infernorum and Ca.* M. limnetica. Direct threading was used to avoid modelling using earlier erroneously modelled Pmo structures (PDB IDs: 1YEW and 3CHX) present in the PDB.

Analysis of community composition and diversity. Bacterial and archaeal community composition was determined from the pre-processed metagenomic reads with SingleM v0.12.1 (https://github.com/wwood/singlem). In total, 28 HMM searches were performed against 14 single-copy ribosomal marker genes. The gene for single-copy ribosomal protein L16/L10E (*rplP*) was selected for downstream analysis and sequences were clustered *de novo* into operational taxonomic units at a sequence identity threshold of 97%. Taxonomic assignment was carried out using the Genome Taxonomy Database [84]. Community richness and beta diversity were calculated using the phyloseq [106] and R package VEGAN [107]. To account for differences in richness between samples, all sequences were rarefied to within 90% of the minimum sequence count. Observed richness and estimated richness (Chao1) were calculated. First, beta diversity (Bray-Curtis) was calculated and visualised using a multidimensional scaling ordination (MDS), then significance testing was carried out using a permutational analysis of variance (PERMANOVA) to test for significant differences in community structure between ecosystems and between depth profiles. A beta dispersion test (PERMDISP) was used to ascertain if significant differences in community structure were due to data dispersion.

Thermodynamic modelling. Cell-specific power (i.e. Gibbs energy per unit time per microbial cell), P (W), was calculated for each reaction using measured *ex situ* oxidation rates according to:

$$P = \frac{r \cdot \Delta G_r}{B} \quad \text{(EQ. 4)}$$

where r denotes the rate of reaction (mol s^{-1} $g_{dry\ soil}^{-1}$), ΔG_r represents the Gibbs energy of the reaction (J mol^{-1}), and B (cells $g_{dry\ soil}^{-1}$) is the number of microbial cells carrying out each of the following the reactions: H_2 + 0.5 O_2 → H_2O (dihydrogen oxidation); CO + 0.5 O_2 → CO_2 (carbon monoxide oxidation); and CH_4 + 2 O_2 → CO_2 +2 H_2O (methane oxidation). Values of ΔG_r are calculated using:

$$\Delta G_r = \Delta G_r^0 + RT \ln Q_r \quad \text{(EQ. 5)}$$

where ΔG_r^0 and Q_r refer to the standard Gibbs energy and the reaction quotient of the indicated reaction, respectively, R represents the gas constant, and T denotes temperature in Kelvin. Values of ΔG_r^0 were calculated using the revised-HKF equations of state [108–110], the SUPCRT92 software package [111], and thermodynamic data taken from references [109,112–115].

Values of Q_r are calculated for each reaction using:

$$Q_r = \prod a_g^{v_i} \quad \text{(EQ. 6)}$$

where a_i stands for the activity of the i^{th} species and v_i corresponds to the stoichiometric coefficient of the i^{th} species in the reaction of interest. Activities of gas-phase compounds, a_g, were calculated using:

$$a_g = \frac{f_g}{f_g^0} \quad \text{(EQ. 7)}$$

where f_g and f_g^0 designate the fugacity and standard state fugacity of the respective gas. Due to the low temperatures and pressures of soil ecosystems, fugacity coefficients for all gases are one (see [116]). Therefore, partial pressures are equivalent to fugacity since f_g^0 was taken to be 1 bar. Gibbs energy calculations were carried out at 20°C and 1 bar. The concentrations of reactants in the catabolic reactions and reaction rates were measured by gas chromatography as described above.

Estimates of the number of microbial cells carrying out each reaction (*B*) were obtained by calculating the proportion of cells performing a specific catabolic reaction in our 16S rRNA gene copy number dataset, assuming all cells to be active. The proportion of a specific functional community was retrieved from the relative abundance of the individual biomarker genes (encoding the large subunits of group 1c, 1d, 1f, 1h, and 2a [NiFe]-hydrogenase, carbon monoxide dehydrogenase (CoxL), particulate methane monooxygenase (PmoA), and soluble methane monooxygenase (MmoX)) in our metagenomics dataset. An average of 4.2 16S rRNA copies per cell was assumed for cell number estimation [117].

To compare our approach to previous literature, we repeated an earlier attempt to estimate the theoretical maximum population of trace gas oxidizing bacteria from modelled ΔG_r and measured reaction rates [68]:

$$N_t = \frac{N_c}{m_E} \Delta G_r \, r \qquad \text{(EQ. 8)}$$

Here, m_E is a mean maintenance energy at 293K in [kJ (C-mol biomass)$^{-1}$ h^{-1}], estimated from pure-culture data of different metabolisms [63]; Nc is the number of cells per C-mol of biomass (1.4 x 10^{14} cells C-mol^{-1} [68], equivalent to 8.6 x 10^{-14} g C dry cell^{-1}); and r is the trace-gas reaction rate as defined above. The ratio N_t / B (the fraction of the estimated trace gas oxidizing population that can be supported given a specific maintenance energy) is equivalent to dividing cell-specific power by the given maintenance energy, after conversion to W cell^{-1} via N_c:

$$\frac{N_t}{B} = \frac{\frac{N_c}{m_E} \Delta G_r \, r}{B} = \frac{P}{\frac{m_E}{N_c}} \qquad \text{(EQ. 9)}$$

Reporting summary. Further information on research design is available in the Nature Research Reporting Summary linked to this article.

Data Availability

All data supporting the findings of the present study are available. All numerical data used to make figures is provided in **Source Data 1** (XLSX format) and all raw phylogenetic trees are provided in Newick (NWK) format in **Source Data 2** (ZIP format). All metagenomes sequenced for this project can be accessed at the Sequence Read Archive with accession number PRJNA656125 (https://www.ncbi.nlm.nih.gov/bioproject/PRJNA656125) and all metagenome-assembled genomes are available at FigShare (https://figshare.com/articles/dataset/Metagenome_Assembled_Genomes/12782543). All previously sequenced metagenomes and metatranscriptomes analysed in this study are available at NCBI BioProject with the accession numbers listed in **Supplementary Table 2**.

References

1. Fierer, N. Embracing the unknown: disentangling the complexities of the soil microbiome. *Nat. Rev. Microbiol.* **15**, 579 (2017).

2. Bell, T., Newman, J. A., Silverman, B. W., Turner, S. L. & Lilley, A. K. The contribution of species richness and composition to bacterial services. *Nature* **436**, 1157 (2005).

3. Delgado-Baquerizo, M. *et al.* A global atlas of the dominant bacteria found in soil. *Science* **359**, 320–325 (2018).

4. Bahram, M. *et al.* Structure and function of the global topsoil microbiome. *Nature* **560**, 233–237 (2018).

5. Jones, S. E. & Lennon, J. T. Dormancy contributes to the maintenance of microbial diversity. *Proc. Natl. Acad. Sci. U. S. A.* **107**, 5881–5886 (2010).

6. Lennon, J. T. & Jones, S. E. Microbial seed banks: the ecological and evolutionary implications of dormancy. *Nat. Rev. Microbiol.* **9**, 119–130 (2011).

7. Schimel, J. & Schaeffer, S. M. Microbial control over carbon cycling in soil. *Front. Microbiol.* **3**, 348 (2012).

8. Janssen, P. H. Identifying the dominant soil bacterial taxa in libraries of 16S rRNA and 16S rRNA genes. *Appl. Environ. Microbiol.* **72**, 1719–1728 (2006).

9. Joseph, S. J., Hugenholtz, P., Sangwan, P., Osborne, C. A. & Janssen, P. H. Laboratory cultivation of widespread and previously uncultured soil bacteria. *Appl. Environ. Microbiol.* **69**, 7210–7215 (2003).

10. Conrad, R. Soil microorganisms as controllers of atmospheric trace gases (H_2, CO, CH_4, OCS, N_2O, and NO). *Microbiol. Rev.* **60**, 609–640 (1996).

11. Beeckman, F., Motte, H. & Beeckman, T. Nitrification in agricultural soils: impact, actors and mitigation. *Curr. Opin. Biotechnol.* **50**, 166–173 (2018).

12. Khdhiri, M. *et al.* Soil carbon content and relative abundance of high affinity H_2-oxidizing bacteria predict atmospheric H_2 soil uptake activity better than soil microbial community composition. *Soil Biol. Biochem.* **85**, 1–9 (2015).

13. Ehhalt, D. H. & Rohrer, F. The tropospheric cycle of H_2: a critical review. *Tellus B* **61**, 500–535 (2009).

14. Novelli, P. C., Masarie, K. A., Tans, P. P. & Lang, P. M. Recent changes in atmospheric carbon monoxide. *Science* **263**, 1587–1590 (1994).

15. Novelli, P. C., Masarie, K. A. & Lang, P. M. Distributions and recent changes of carbon monoxide in the lower troposphere. *J. Geophys. Res. Atmos.* **103**, 19015–19033 (1998).

16. Kirschke, S. *et al.* Three decades of global methane sources and sinks. *Nat. Geosci* **6**, 813–823 (2013).

17. Constant, P., Poissant, L. & Villemur, R. Tropospheric H_2 budget and the response of its soil uptake under the changing environment. *Sci. Total Environ.* **407**, 1809–1823 (2009).

18. Berney, M., Greening, C., Conrad, R., Jacobs, W. R. & Cook, G. M. An obligately aerobic soil bacterium activates fermentative hydrogen production to survive reductive stress during hypoxia. *Proc. Natl. Acad. Sci. U. S. A.* **111**, 11479–11484 (2014).

19. Tarr, M. A., Miller, W. L. & Zepp, R. G. Direct carbon monoxide photoproduction from plant matter. *J. Geophys. Res. Atmos.* **100**, 11403–11413 (1995).

20. King, G. M. & Weber, C. F. Distribution, diversity and ecology of aerobic CO-oxidizing bacteria. *Nat. Rev. Microbiol.* **5**, 107–118 (2007).

21. Conrad, R. The global methane cycle: recent advances in understanding the microbial processes involved. *Environ. Microbiol. Rep.* **1**, 285–292 (2009).

22. Constant, P., Chowdhury, S. P., Pratscher, J. & Conrad, R. Streptomycetes contributing to atmospheric molecular hydrogen soil uptake are widespread and encode a putative high-affinity [NiFe]-hydrogenase. *Environ. Microbiol.* **12**, 821–829 (2010).

23. Greening, C., Berney, M., Hards, K., Cook, G. M. & Conrad, R. A soil actinobacterium scavenges atmospheric H_2 using two membrane-associated, oxygen-dependent [NiFe] hydrogenases. *Proc. Natl. Acad. Sci. U. S. A.* **111**, 4257–4261 (2014).

24. Cordero, P. R. F. *et al.* Atmospheric carbon monoxide oxidation is a widespread mechanism supporting microbial survival. *ISME J.* **13**, 2868–2881 (2019).

25. Mörsdorf, G., Frunzke, K., Gadkari, D. & Meyer, O. Microbial growth on carbon monoxide. *Biodegradation* **3**, 61–82 (1992).

26. Greening, C. *et al.* Genomic and metagenomic surveys of hydrogenase distribution indicate H_2 is a widely utilised energy source for microbial growth and survival. *ISME J.* **10**, 761–777 (2016).

27. Tveit, A. T. *et al.* Widespread soil bacterium that oxidizes atmospheric methane. *Proc. Natl. Acad. Sci. U. S. A.* **116**, 8515–8524 (2019).

28. Islam, Z. F. *et al.* A widely distributed hydrogenase oxidises atmospheric H_2 during

bacterial growth. *ISME J.* 10.1038/s41396-020-0713–4 (2020).

29. King, G. M. Molecular and culture-based analyses of aerobic carbon monoxide oxidizer diversity. ***Appl. Environ. Microbiol.* 69**, 7257–7265 (2003).

30. Greening, C. ***et al.*** Persistence of the dominant soil phylum Acidobacteria by trace gas scavenging. ***Proc. Natl. Acad. Sci. U. S. A.* 112**, 10497–10502 (2015).

31. Berney, M. & Cook, G. M. Unique flexibility in energy metabolism allows mycobacteria to combat starvation and hypoxia. *PLoS One* **5**, e8614 (2010).

32. Greening, C., Villas-Bôas, S. G., Robson, J. R., Berney, M. & Cook, G. M. The growth and survival of *Mycobacterium smegmatis* is enhanced by co-metabolism of atmospheric H_2. *PLoS One* **9**, e103034 (2014).

33. Liot, Q. & Constant, P. Breathing air to save energy – new insights into the ecophysiological role of high-affinity [NiFe]-hydrogenase in Streptomyces avermitilis. *Microbiologyopen* **5**, 47–59 (2016).

34. Greening, C., Grinter, R. & Chiri, E. Uncovering the metabolic strategies of the dormant microbial majority: towards integrative approaches. *mSystems* **4**, e00107-19 (2019).

35. Khdhiri, M., Piché-Choquette, S., Tremblay, J., Tringe, S. G. & Constant, P. Meta-omics survey of [NiFe]-hydrogenase genes fails to capture drastic variations in H_2-oxidation activity measured in three soils exposed to H_2. ***Soil Biol. Biochem.* 125**, 239–243 (2018).

36. Quiza, L., Lalonde, I., Guertin, C. & Constant, P. Land-use influences the distribution and activity of high affinity CO-oxidizing bacteria Associated to type I-coxL genotype in soil. ***Front. Microbiol.* 5**, 271 (2014).

37. Ji, M. ***et al.*** Atmospheric trace gases support primary production in Antarctic desert surface soil. *Nature* **552**, 400–403 (2017).

38. Lynch, R. C., Darcy, J. L., Kane, N. C., Nemergut, D. R. & Schmidt, S. K. Metagenomic evidence for metabolism of trace atmospheric gases by high-elevation desert Actinobacteria. ***Front. Microbiol.* 5**, 698 (2014).

39. King, G. M. Contributions of atmospheric CO and hydrogen uptake to microbial dynamics on recent Hawaiian volcanic deposits. ***Appl. Environ. Microbiol.* 69**, 4067–4075 (2003).

40. Cordero, P. R. F. ***et al.*** Carbon monoxide dehydrogenases enhance bacterial survival by respiring atmospheric CO. *bioRxiv* 628081 (2019) doi:10.1101/628081.

41. Constant, P., Chowdhury, S. P., Hesse, L., Pratscher, J. & Conrad, R. Genome data mining and soil survey for the novel Group 5 [NiFe]-hydrogenase to explore the diversity and ecological importance of presumptive high-affinity H_2-oxidizing bacteria. ***Appl. Environ. Microbiol.* 77**, 6027–6035 (2011).

42. Pandelia, M. E., Lubitz, W. & Nitschke, W. Evolution and diversification of Group 1 [NiFe] hydrogenases. Is there a phylogenetic marker for O_2-tolerance? ***Biochim. Biophys. Acta - Bioenerg.* 1817**, 1565–1575 (2012).

43. Myers, M. R. & King, G. M. Isolation and characterization of *Acidobacterium ailaaui* sp. nov., a novel member of Acidobacteria subdivision 1, from a geothermally heated

Hawaiian microbial mat. *Int. J. Syst. Evol. Microbiol.* **66**, 5328–5335 (2016).

44. Cunliffe, M. Correlating carbon monoxide oxidation with cox genes in the abundant marine *Roseobacter* clade. *ISME J.* **5**, 685 (2011).

45. van Kessel, M. A. H. J. *et al.* Complete nitrification by a single microorganism. *Nature* **528**, 555 (2015).

46. Daims, H. *et al.* Complete nitrification by *Nitrospira* bacteria. *Nature* **528**, 504 (2015).

47. Knief, C. Diversity and habitat preferences of cultivated and uncultivated aerobic methanotrophic bacteria evaluated based on *pmoA* as molecular marker. *Front. Microbiol.* **6**, 1346 (2015).

48. Chiri, E. *et al.* Termite mounds contain soil-derived methanotroph communities kinetically adapted to elevated methane concentrations. *ISME J.* 1–17 (2020).

49. Dunfield, P. F. *et al.* Methane oxidation by an extremely acidophilic bacterium of the phylum Verrucomicrobia. *Nature* **450**, 879–882 (2007).

50. Haroon, M. F. *et al.* Anaerobic oxidation of methane coupled to nitrate reduction in a novel archaeal lineage. *Nature* **500**, 567–70 (2013).

51. Khadka, R. *et al.* Evolutionary history of copper membrane monooxygenases. *Front. Microbiol.* **9**, 2493 (2018).

52. Van Asperen, H. *et al.* The role of photo-and thermal degradation for CO_2 and CO fluxes in an arid ecosystem. *Biogeosciences* **12**, (2015).

53. Moxley, J. M. & Smith, K. A. Carbon monoxide production and emission by some Scottish soils. *Tellus B Chem. Phys. Meteorol.* **50**, 151–162 (1998).

54. Dutaur, L. & Verchot, L. V. A global inventory of the soil CH_4 sink. *Global Biogeochem. Cycles* **21**, GB4013 (2007).

55. McLearn, N. & Dong, Z. Microbial nature of the hydrogen-oxidizing agent in hydrogen-treated soil. *Biol. Fertil. Soils* **35**, 465–469 (2002).

56. King, G. M. Attributes of atmospheric carbon monoxide oxidation by Maine forest soils. *Appl. Environ. Microbiol.* **65**, 5257–5264 (1999).

57. Kolb, S., Knief, C., Dunfield, P. F. & Conrad, R. Abundance and activity of uncultured methanotrophic bacteria involved in the consumption of atmospheric methane in two forest soils. *Environ. Microbiol.* **7**, 1150–1161 (2005).

58. Priemé, A. & Christensen, S. Seasonal and spatial variation of methane oxidation in a Danish spruce forest. *Soil Biol. Biochem.* **29**, 1165–1172 (1997).

59. Chen, Q., Popa, M. E., Batenburg, A. M. & Röckmann, T. Isotopic signatures of production and uptake of H_2 by soil. *Atmos. Chem. Phys.* **15**, 13003–13021 (2015).

60. DeLong, J. P., Okie, J. G., Moses, M. E., Sibly, R. M. & Brown, J. H. Shifts in metabolic scaling, production, and efficiency across major evolutionary transitions of life. *Proc. Natl. Acad. Sci.* **107**, 12941–12945 (2010).

839 61. Kempes, C. P. *et al.* Drivers of bacterial maintenance and minimal energy requirements.
840 *Front. Microbiol.* **8**, 31 (2017).

841 62. Marschall, E., Jogler, M., Henßge, U. & Overmann, J. Large□scale distribution and
842 activity patterns of an extremely low□light□adapted population of green sulfur bacteria in
843 the Black Sea. *Environ. Microbiol.* **12**, 1348–1362 (2010).

844 63. Tijhuis, L., Van Loosdrecht, M. C. & Heijnen, J. J. A thermodynamically based
845 correlation for maintenance gibbs energy requirements in aerobic and anaerobic
846 chemotrophic growth. *Biotechnol. Bioeng.* **42**, 509–519 (1993).

847 64. LaRowe, D. E. & Amend, J. P. Power limits for microbial life. *Front. Microbiol.* **6**, 718
848 (2015).

849 65. Bradley, J. A. *et al.* Widespread energy limitation to life in global subseafloor sediments.
850 *Sci. Adv.* **6**, eaba0697 (2020).

851 66. Røy, H. *et al.* Aerobic microbial respiration in 86-million-year-old deep-sea red clay.
852 *Science* **336**, 922–925 (2012).

853 67. Conrad, R. Capacity of aerobic microorganisms to utilize and grow on atmospheric trace
854 gases (H_2, CO, CH_4). in *Current Perspectives in Microbial Ecology* (eds. Klug, M. G. &
855 Reddy, C. A.) 461–467 (American Society for Microbiology, 1984).

856 68. Conrad, R. Soil microorganisms oxidizing atmospheric trace gases (CH_4, CO, H_2, NO).
857 *Indian J. Microbiol.* **39**, 193–203 (1999).

858 69. Meredith, L. K. *et al.* Ecosystem fluxes of hydrogen in a mid□latitude forest driven by
859 soil microorganisms and plants. *Glob. Chang. Biol.* **23**, 906–919 (2017).

860 70. Carini, P. *et al.* Relic DNA is abundant in soil and obscures estimates of soil microbial
861 diversity. *Nat. Microbiol.* **2**, 1–6 (2016).

862 71. Schmitz, R. A. *et al.* The thermoacidophilic methanotroph *Methylacidiphilum*
863 *fumariolicum* SolV oxidizes subatmospheric H_2 with a high-affinity, membrane-associated
864 [NiFe] hydrogenase. *ISME J.* **14**, 1223–1232 (2020).

865 72. Islam, Z. F. *et al.* Two Chloroflexi classes independently evolved the ability to persist on
866 atmospheric hydrogen and carbon monoxide. *ISME J.* **13**, 1801–1813 (2019).

867 73. Hüppi, R. *et al.* Restricting the nonlinearity parameter in soil greenhouse gas flux
868 calculation for more reliable flux estimates. *PLoS One* **13**, (2018).

869 74. Caporaso, J. G. *et al.* Global patterns of 16S rRNA diversity at a depth of millions of
870 sequences per sample. *Proc. Natl. Acad. Sci. U. S. A.* **108**, 4516–4522 (2011).

871 75. Uritskiy, G. V, DiRuggiero, J. & Taylor, J. MetaWRAP—a flexible pipeline for genome-
872 resolved metagenomic data analysis. *Microbiome* **6**, 158 (2018).

873 76. Li, D., Liu, C.-M., Luo, R., Sadakane, K. & Lam, T.-W. MEGAHIT: an ultra-fast single-
874 node solution for large and complex metagenomics assembly via succinct de Bruijn graph.
875 *Bioinformatics* **31**, 1674–1676 (2015).

876 77. Nurk, S., Meleshko, D., Korobeynikov, A. & Pevzner, P. A. metaSPAdes: a new versatile

metagenomic assembler. *Genome Res.* **27**, 824–834 (2017).

78. Kang, D. D., Froula, J., Egan, R. & Wang, Z. MetaBAT, an efficient tool for accurately reconstructing single genomes from complex microbial communities. *PeerJ* **3**, e1165 (2015).

79. Kang, D. *et al.* MetaBAT 2: an adaptive binning algorithm for robust and efficient genome reconstruction from metagenome assemblies. *PeerJ* **7**, e7359 (2019).

80. Wu, Y.-W., Simmons, B. A. & Singer, S. W. MaxBin 2.0: an automated binning algorithm to recover genomes from multiple metagenomic datasets. *Bioinformatics* **32**, 605–607 (2015).

81. Olm, M. R., Brown, C. T., Brooks, B. & Banfield, J. F. dRep: a tool for fast and accurate genomic comparisons that enables improved genome recovery from metagenomes through de-replication. *ISME J.* **11**, 2864 (2017).

82. Parks, D. H., Imelfort, M., Skennerton, C. T., Hugenholtz, P. & Tyson, G. W. CheckM: assessing the quality of microbial genomes recovered from isolates, single cells, and metagenomes. *Genome Res.* **25**, 1043–1055 (2015).

83. Bowers, R. M. *et al.* Minimum information about a single amplified genome (MISAG) and a metagenome-assembled genome (MIMAG) of bacteria and archaea. *Nat. Biotechnol.* **35**, 725–731 (2017).

84. Parks, D. H. *et al.* A standardized bacterial taxonomy based on genome phylogeny substantially revises the tree of life. *Nat. Biotechnol.* **36**, 996–1004 (2018).

85. Chaumeil, P.-A., Mussig, A. J., Hugenholtz, P. & Parks, D. H. GTDB-Tk: a toolkit to classify genomes with the Genome Taxonomy Database. *Bioinformatics* **36**, 1925–1927 (2020).

86. Markowitz, V. M. *et al.* IMG: the integrated microbial genomes database and comparative analysis system. *Nucleic Acids Research* vol. 40 D115-22 (2012).

87. Leinonen, R., Sugawara, H., Shumway, M. & Collaboration, I. N. S. D. The sequence read archive. *Nucleic Acids Res.* **39**, D19–D21 (2010).

88. Jansson, J. K. Next generation ecosystem experiment (NGEE) in the Arctic. (2013) doi:10.25585/1487743.

89. Constant, P. Metagenomic and metatranscriptomic analysis of soil biogeochemical processes sustained by interspecific transfer of molecular hydrogen. (2014) doi:10.25585/1487738.

90. Tiedje, J. M. Metagenomic analysis of the rhizosphere of three biofuel crops at the KBS intensive site. (2013) doi:10.25585/1488010.

91. Mohn, W. W. Metagenomic and metatranscriptomic analysis of forest soil communities across North America. (2012) doi:10.25585/1487719.

92. Kalyuzhnaya, M. G. Systems level insights into methane cycling in arid and semi-arid ecosystems via community metagenomics and metatranscriptomics. (2016) doi:10.25585/1488146.

93. Cadillo-Quiroz, H. Microbial composition and metagenomic functional potential across Tropical Peatlands: comparative evaluation and modeling of C decomposition to greenhouse gases. (2015) doi:10.25585/1488117.

94. Oliveira, R. Unravelling microbial communities associated with native plant species from P-impoverished soils of a global biodiversity hotspot. (2017) doi:10.25585/1488283.

95. Pett-Ridge, J. Microbial carbon transformations in wet tropical soils: effects of redox fluctuation. (2017) doi:10.25585/1488160.

96. Hyatt, D. *et al.* Prodigal: prokaryotic gene recognition and translation initiation site identification. *BMC Bioinformatics* **11**, 119 (2010).

97. Buchfink, B., Xie, C. & Huson, D. H. Fast and sensitive protein alignment using DIAMOND. *Nat. Methods* **12**, 59 (2014).

98. Anantharaman, K. *et al.* Thousands of microbial genomes shed light on interconnected biogeochemical processes in an aquifer system. *Nat. Commun.* **7**, 13219 (2016).

99. Altschul, S. F., Gish, W., Miller, W., Myers, E. W. & Lipman, D. J. Basic local alignment search tool. *J. Mol. Biol.* **215**, 403–410 (1990).

100. Kopylova, E., Noé, L. & Touzet, H. SortMeRNA: fast and accurate filtering of ribosomal RNAs in metatranscriptomic data. *Bioinformatics* **28**, 3211–3217 (2012).

101. Patro, R., Duggal, G., Love, M. I., Irizarry, R. A. & Kingsford, C. Salmon provides fast and bias-aware quantification of transcript expression. *Nat. Methods* **14**, 417–419 (2017).

102. Fu, L., Niu, B., Zhu, Z., Wu, S. & Li, W. CD-HIT: accelerated for clustering the next-generation sequencing data. *Bioinformatics* **28**, 3150–3152 (2012).

103. Kumar, S., Stecher, G. & Tamura, K. MEGA7: Molecular Evolutionary Genetics Analysis version 7.0 for bigger datasets. *Mol. Biol. Evol.* msw054 (2016).

104. Kelley, L. A., Mezulis, S., Yates, C. M., Wass, M. N. & Sternberg, M. J. E. The Phyre2 web portal for protein modeling, prediction and analysis. *Nat. Protoc.* **10**, 845–858 (2015).

105. Smith, S. M. *et al.* Crystal structure and characterization of particulate methane monooxygenase from *Methylocystis* species strain M. *Biochemistry* **50**, 10231–10240 (2011).

106. McMurdie, P. J. & Holmes, S. phyloseq: an R package for reproducible interactive analysis and graphics of microbiome census data. *PLoS One* **8**, e61217 (2013).

107. Dixon, P. VEGAN, a package of R functions for community ecology. *J. Veg. Sci.* **14**, 927–930 (2003).

108. Helgeson, H., Kirkham, D. & Flowers, G. Theoretical prediction of the thermodynamic behavior of aqueous electrolytes by high pressures and temperatures; IV, Calculation of activity coefficients, osmotic coefficients, and apparent molal and standard and relative partial molal properties to 600 d. *Am. J. Sci.* **281**, 1249–1516 (1981).

109. Shock, E. L. & Helgeson, H. C. Calculation of the thermodynamic and transport properties of aqueous species at high pressures and temperatures: Correlation algorithms

for ionic species and equation of state predictions to 5 kb and 1000°C. *Geochim. Cosmochim. Acta* **52**, 2009–2036 (1988).

110. Shock, E. L. (University of C. at B., Oelkers, E. H., Johnson, J. W., Sverjensky, D. A. & Helgeson, H. C. Calculation of the thermodynamic properties of aqueous Species at high pressures and temperatures. *J. Chem. Soc. Faraday Trans.* **88**, 803–826 (1992).

111. Johnson, J. W., Oelkers, E. H. & Helgeson, H. C. A software package for calculating the standard molal thermodynamic properties of minerals, gases, aqueous species and reactions from 1 to 5000 bars and 0° to 1000° C. *Comput. Geosci.* **18**, 899–947 (1992).

112. Shock, E. L., Helgeson, H. C. & Sverjensky, D. A. Calculation of the thermodynamic and transport properties of aqueous species at high pressures and temperatures: Standard partial molal properties of inorganic neutral species. *Geochim. Cosmochim. Acta* **53**, 2157–2183 (1989).

113. Shock, E. L. & Helgeson, H. C. Calculation of the thermodynamic and transport properties of aqueous species at high pressures and temperatures: Standard partial molal properties of organic species. *Geochim. Cosmochim. Acta* **54**, 915–945 (1990).

114. Sverjensky, D. A., Shock, E. L. & Helgeson, H. C. Prediction of the thermodynamic properties of aqueous metal complexes to 1000°C and 5 kb. *Geochim. Cosmochim. Acta* **61**, 1359–1412 (1997).

115. Schulte, M. D., Shock, E. L. & Wood, R. H. The temperature dependence of the standard-state thermodynamic properties of aqueous nonelectrolytes. *Geochim. Cosmochim. Acta* **65**, 3919–3930 (2001).

116. Amend, J. P. & LaRowe, D. E. Minireview: demystifying microbial reaction energetics. *Environ. Microbiol.* **21**, 3539–3547 (2019).

117. Větrovský, T. & Baldrian, P. The variability of the 16S rRNA gene in bacterial genomes and its consequences for bacterial community analyses. *PLoS One* **8**, e57923 (2013).

Acknowledgements

This research was supported by an Australian Research Council DECRA Fellowship (DE170100310; C.G.), a Discovery Project grant (DP180101762; C.G. and P.L.M.C.), a Swiss National Foundation Early Mobility Postdoctoral Fellowship (P2EZP3_178421; E.C.), a NSFC grant (41906076; X.D.), a NERC grant (NE/T010967/1; J.B.), a Humboldt Foundation Fellowship (J.B.), Monash University PhD scholarships (S.K.B. and P.M.L.), and an NHMRC EL2 Fellowship (APP1178715; salary for C.G.). We thank Maria Chuvochina for etymological advice, Steven Chown, Sergio Morales, Matthew Stott, and Gregory Cook for formative discussions, and the four reviewers for their helpful suggestions.

Author information

Contributions

C.G. conceived and supervised this study. S.K.B., C.G., E.C., and P.A.N. designed experiments and analyzed data. Different authors were responsible for performing fieldwork (S.K.B., E.C., P.M.L., C.G.), laboratory work (S.K.B., T.J., E.C.), metagenome assembly (X.D.), metagenome analysis (S.K.B., C.G., X.D., E.C.), phylogenetic analysis (C.G.), protein modelling (R.G.), and thermodynamic modelling (J.A.B., P.A.N., D.L., E.C., S.K.B.). S.K.A. and P.L.M.C. provided logistical and theoretical support. C.G., S.K.B., and P.A.N. wrote the paper with input from all authors.

Corresponding authors

Correspondence to Chris Greening (chris.greening@monash.edu) and Eleonora Chiri (eleonora.chiri@monash.edu).

Ethics declarations

Competing interests

The authors declare no competing financial interests.

Additional information

Etymological Information

Candidatus Methylotropicum (Me.thy.lo.tro'pi.cum.) N.L. n. *methylum* (from French *méthyle* back-formation from French *méthylène*, coined from Gr. n. *methu*, wine and Gr. n. *hulê*, wood), the methyl group; N.L. pref. *methylo-*, pertaining to the methyl radical; L. masc. adj. *tropicus* pertaining to tropical zone of the Earth; N.L. neut. n. *Methylotropicum* referring to a methyl-using bacterium from the tropics. *Candidatus* Methylotropicum kingii (ki'ngi.i.) N.L. gen. n. *kingii* in honor of Prof. Gary King, who has pioneered research into the microbial oxidation of methane, CO, and H_2.

Figure legends

Fig. 1. Energy conservation and carbon acquisition strategies of global soil bacteria. Homology-based searches were used to detect marker genes for key metabolic processes in the metagenomic short reads and metagenome-assembled genomes. **(a)** Heatmaps showing the abundance of each gene in the metagenomic short reads of the four Australian depth profiles and eight global sites. The percentage of the total community predicted to encode at least one of each gene for a process is shown, based on normalization to single-copy marker genes. The genes detected are usually present in single copies in genomes and, where genes performing similar functions are collapsed together, the values are summed up to 100%. **(b)** Dot plot showing the metabolic potential of the 757 metagenome-assembled genomes (MAGs). The size of each point represents the number of genomes in each phylum that encode the gene of interest and the shading represents the average genome completeness. Taxonomy assignment is based on the Genome Taxonomy Database (GTDB) [52].

Fig. 2. Radial maximum-likelihood phylogenetic trees showing the sequence diversity and taxonomic distribution of key enzymes associated with trace gas oxidation. The trees show the amino acid sequences of **(a)** group 1 and 2 [NiFe]-hydrogenase large subunits and **(b)** form I [MoCu]-carbon monoxide dehydrogenase large subunit (CoxL). The tree shows sequences from the soil metagenome-assembled genomes (taxa names colored by phylum; 167 hydrogenase sequences, 141 CO dehydrogenase sequences) alongside representative sequences from NCBI reference genomes (taxa names shown in grey; 168 hydrogenase sequences, 171 CO dehydrogenase sequences). The hydrogenase subgroups and carbon monoxide dehydrogenase clades predicted to support trace gas oxidation in the sampled soils are highlighted. Both trees were constructed using the JTT matrix-based model, used all sites, and were bootstrapped with 50 replicates. Source data is provided in Newick (nwk) format.

Fig. 3. Measurement of oxidation of the trace gases H_2, CO, and CH_4 across four Australian soil ecosystems. **(a)** Depth-resolved *in situ* gas concentrations from 0 to 16 cm depth at each ecosystem (wetland, grassland, forest, dryland). **(b)** *In situ* soil-atmosphere gas fluxes (J_{atm}; positive values indicate net gas production, negative values indicate net gas consumption). Dashed lines represent upper and lower simulated flux detection limits, with most CO and CH_4 flux values falling within them. For **a** and **b**, measurements were performed in four separate soils per biome and error bars showing standard deviations. **(c)** Depth-resolved, cell-specific *ex situ* oxidation rates for each ecosystem of core samples from four different depths (0-5, 5-10, 15-20,

25-30 cm). Measurements were performed with four biological replicates for each soil ecosystem and treatment (dryland wet). Oxidation rate values are normalized to total predicted cell number of trace gas oxidizers based on 16S rRNA gene qPCR and percentage of the community predicted to oxidize each gas. **(d)** Amount of power per cell derived from the oxidation of each trace gas. These were calculated using thermodynamic models based on *ex situ* rates measured across the four depths per habitat. The colored bars depict the range of literature values of maintenance energy requirements or endogenous metabolic rates of different pure cultures (green [63], yellow [64], blue [60]) and hydrogen oxidizers in deep marine sediments (pink [64,65]). For **c** and **d**, boxplots show means, lower and upper quartile, and minimum and maximum values.

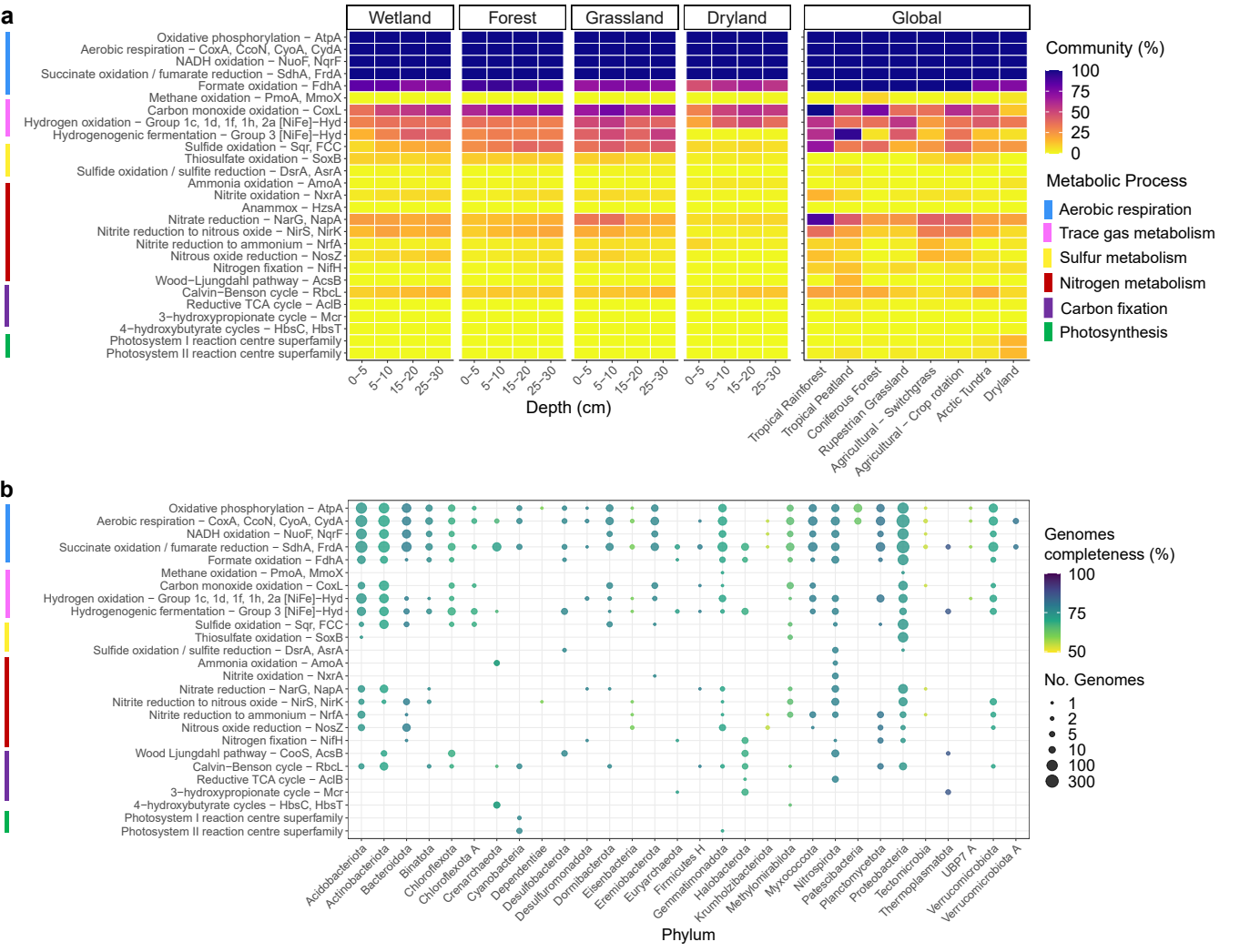
a
Wetland
Forest
Grassland
Dryland
Global
Oxidative phosphorylation − AtpA
Aerobic respiration − CoxA, CcoN, CyoA, CydA
NADH oxidation − NuoF, NqrF
Succinate oxidation / fumarate reduction − SdhA, FrdA
Formate oxidation − FdhA
Methane oxidation − PmoA, MmoX
Carbon monoxide oxidation − CoxL
Hydrogen oxidation − Group 1c, 1d, 1f, 1h, 2a [NiFe]−Hyd
Hydrogenogenic fermentation − Group 3 [NiFe]−Hyd
Sulfide oxidation − Sqr, FCC
Thiosulfate oxidation − SoxB
Sulfide oxidation / sulfite reduction − DsrA, AsrA
Ammonia oxidation − AmoA
Nitrite oxidation − NxrA
Anammox − HzsA
Nitrate reduction − NarG, NapA
Nitrite reduction to nitrous oxide − NirS, NirK
Nitrite reduction to ammonium − NrfA
Nitrous oxide reduction − NosZ
Nitrogen fixation − NifH
Wood−Ljungdahl pathway − AcsB
Calvin−Benson cycle − RbcL
Reductive TCA cycle − AclB
3−hydroxypropionate cycle − Mcr
4−hydroxybutyrate cycles − HbsC, HbsT
Photosystem I reaction centre superfamily
Photosystem II reaction centre superfamily
0–5
5–10
15–20
25–30
Depth (cm)
Tropical Rainforest
Tropical Peatland
Coniferous Forest
Rupestrian Grassland
Agricultural − Switchgrass
Agricultural − Crop rotation
Arctic Tundra
Dryland
Community (%)
100
75
50
25
0
Metabolic Process
Aerobic respiration
Trace gas metabolism
Sulfur metabolism
Nitrogen metabolism
Carbon fixation
Photosynthesis
b
Genomes completeness (%)
100
75
50
No. Genomes
1
2
5
10
100
300
Acidobacteriota
Actinobacteriota
Bacteroidota
Binatota
Chloroflexota
Chloroflexota A
Crenarchaeota
Cyanobacteria
Dependentiae
Desulfobacterota
Desulfuromonadota
Dormibacterota
Eisenbacteria
Eremiobacterota
Euryarchaeota
Firmicutes H
Gemmatimonadota
Halobacteriota
Krumholzibacteriota
Methylomirabilota
Myxococcota
Nitrospirota
Patescibacteria
Planctomycetota
Proteobacteria
Tectomicrobia
Thermoplasmatota
UBP7 A
Verrucomicrobiota
Verrucomicrobiota A
Phylum

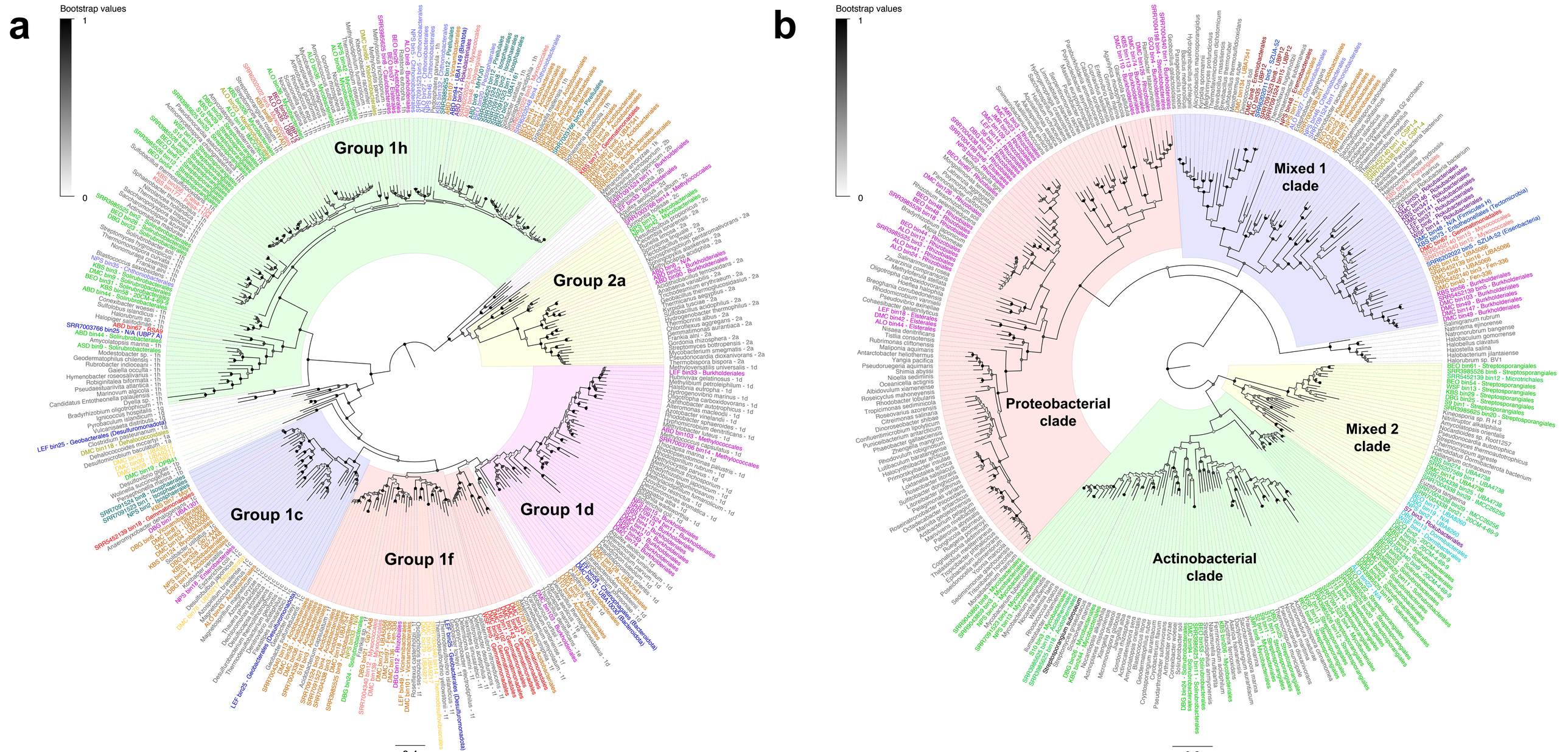
a
Bootstrap values
1
0
Group 1h
Group 2a
Group 1d
Group 1c
Group 1f
0.4
b
Bootstrap values
1
0
Mixed 1 clade
Proteobacterial clade
Mixed 2 clade
Actinobacterial clade
0.2
Acidobacteriota
Actinobacteriota
Chloroflexota
Dormibacterota
Eremiobacterota
Gemmatimonadota
Methylomirabilota
Myxococcota
Nitrospirota
Proteobacteria
Planctomycetota
Verrucomicrobiota
Other phyla
Reference sequences

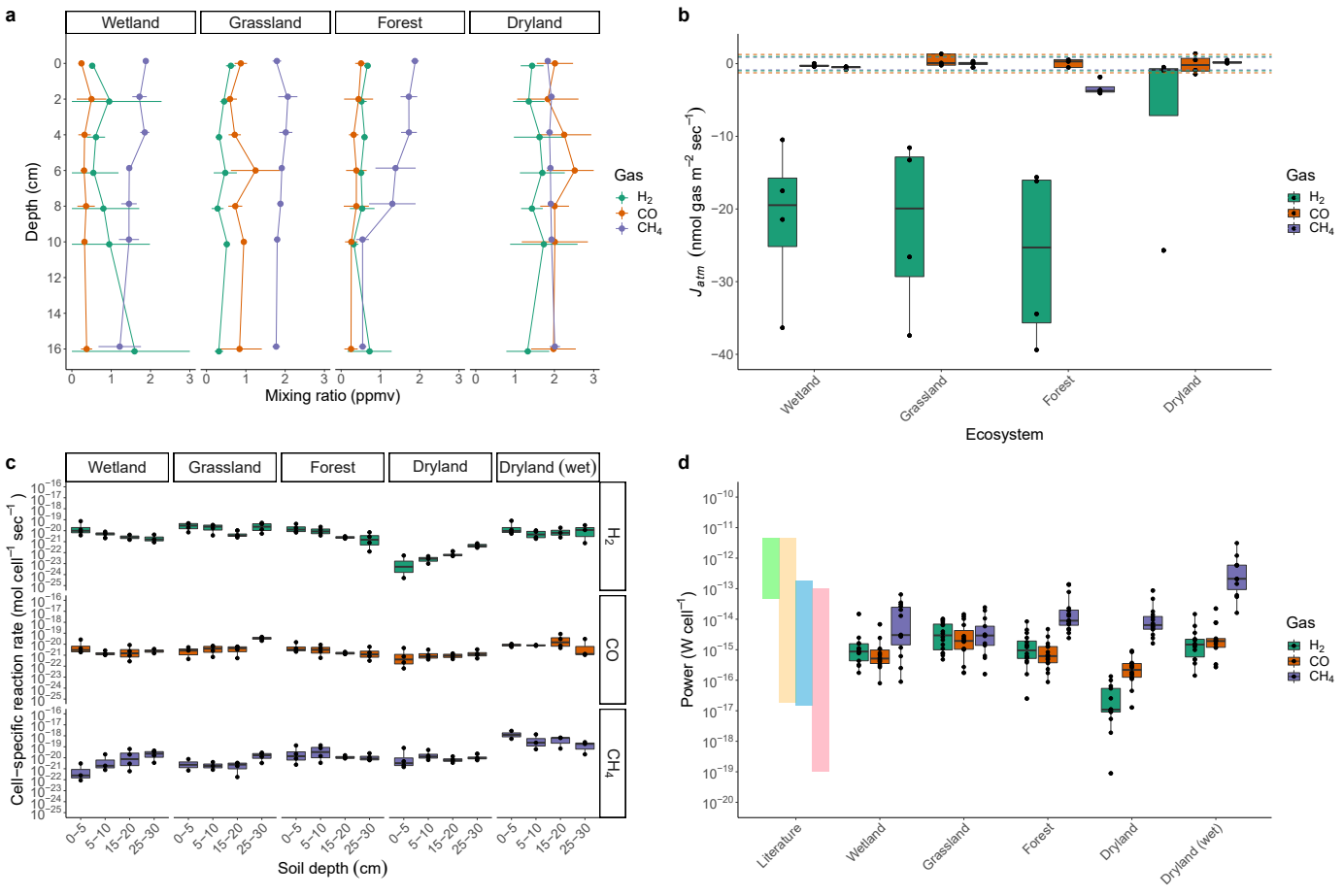
a
Wetland
Grassland
Forest
Dryland
Depth (cm)
Mixing ratio (ppmv)
Gas
H2
CO
CH4
b
Jatm (nmol gas m−2 sec−1)
Wetland
Grassland
Forest
Dryland
Ecosystem
Gas
H2
CO
CH4
c
Wetland
Grassland
Forest
Dryland
Dryland (wet)
H2
CO
CH4
Cell−specific reaction rate (mol cell−1 sec−1)
0–5
5–10
15–20
25–30
Soil depth (cm)
d
Power (W cell−1)
Literature
Wetland
Grassland
Forest
Dryland
Dryland (wet)
Gas
H2
CO
CH4

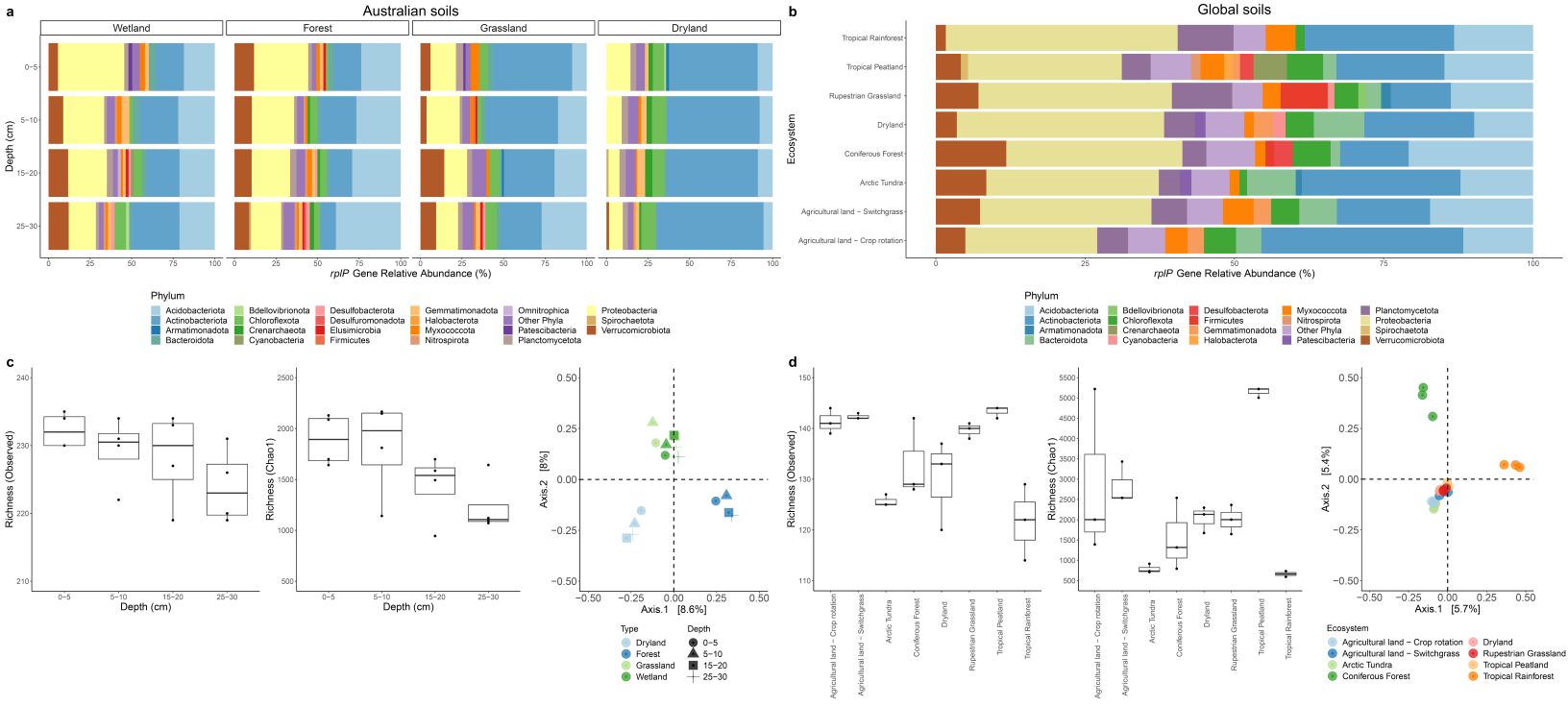
a
Australian soils
Wetland
Forest
Grassland
Dryland
Depth (cm)
0–5
5–10
15–20
25–30
rplP Gene Relative Abundance (%)
b
Global soils
Ecosystem
Tropical Rainforest
Tropical Peatland
Rupestrian Grassland
Dryland
Coniferous Forest
Arctic Tundra
Agricultural land – Switchgrass
Agricultural land – Crop rotation
rplP Gene Relative Abundance (%)
Phylum
Acidobacteriota
Actinobacteriota
Armatimonadota
Bacteroidota
Bdellovibrionota
Chloroflexota
Crenarchaeota
Cyanobacteria
Desulfobacterota
Desulfuromonadota
Elusimicrobia
Firmicutes
Gemmatimonadota
Halobacterota
Myxococcota
Nitrospirota
Omnitrophica
Other Phyla
Patescibacteria
Planctomycetota
Proteobacteria
Spirochaetota
Verrucomicrobiota
c
Richness (Observed)
Depth (cm)
Richness (Chao1)
Axis.2 [8%]
Axis.1 [8.6%]
Type
Dryland
Forest
Grassland
Wetland
Depth
0–5
5–10
15–20
25–30
d
Richness (Observed)
Richness (Chao1)
Axis.2 [5.4%]
Axis.1 [5.7%]
Ecosystem
Agricultural land – Crop rotation
Agricultural land – Switchgrass
Arctic Tundra
Coniferous Forest
Dryland
Rupestrian Grassland
Tropical Peatland
Tropical Rainforest

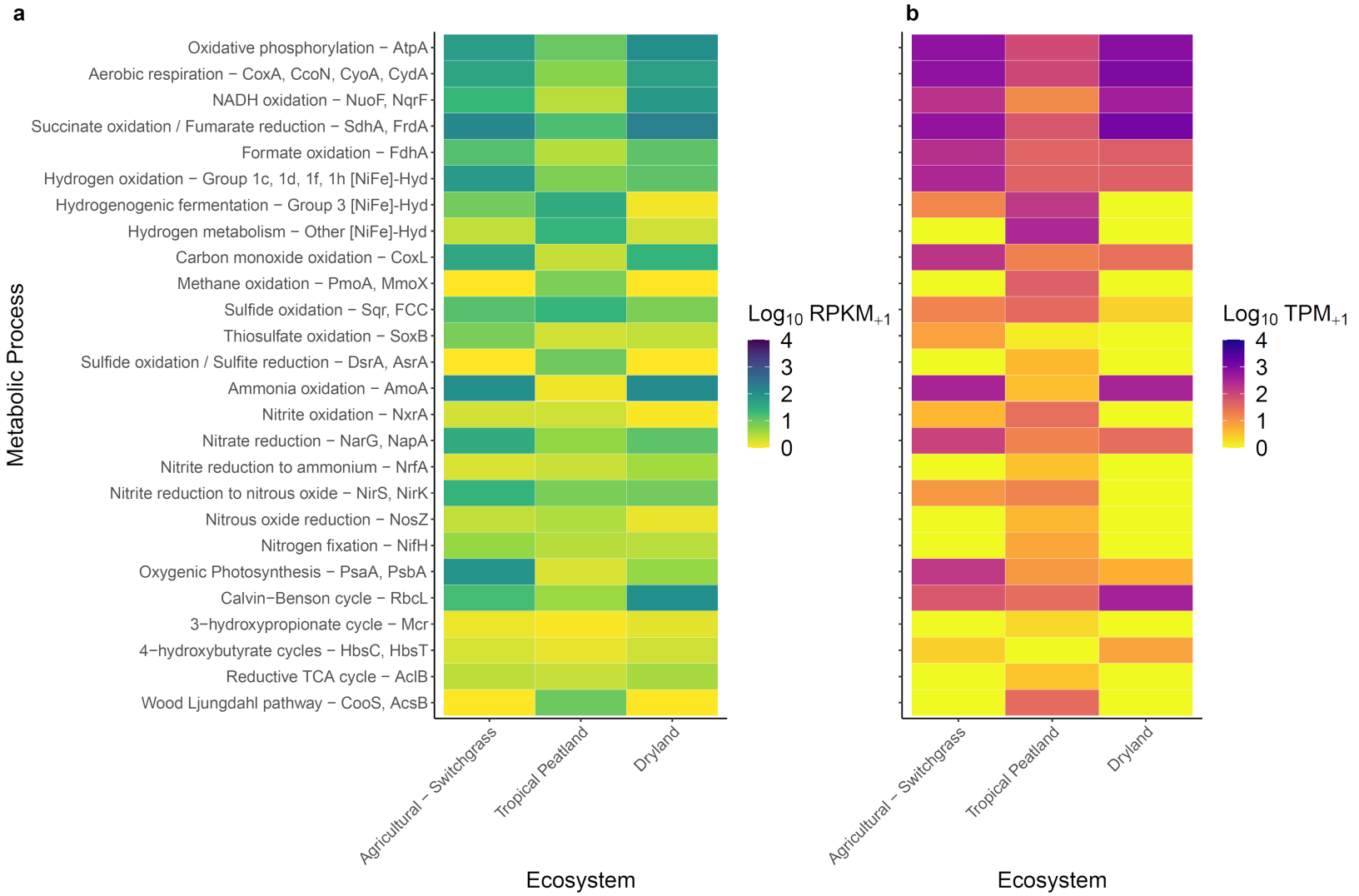
a
b
Metabolic Process
Oxidative phosphorylation − AtpA
Aerobic respiration − CoxA, CcoN, CyoA, CydA
NADH oxidation − NuoF, NqrF
Succinate oxidation / Fumarate reduction − SdhA, FrdA
Formate oxidation − FdhA
Hydrogen oxidation − Group 1c, 1d, 1f, 1h [NiFe]-Hyd
Hydrogenogenic fermentation − Group 3 [NiFe]-Hyd
Hydrogen metabolism − Other [NiFe]-Hyd
Carbon monoxide oxidation − CoxL
Methane oxidation − PmoA, MmoX
Sulfide oxidation − Sqr, FCC
Thiosulfate oxidation − SoxB
Sulfide oxidation / Sulfite reduction − DsrA, AsrA
Ammonia oxidation − AmoA
Nitrite oxidation − NxrA
Nitrate reduction − NarG, NapA
Nitrite reduction to ammonium − NrfA
Nitrite reduction to nitrous oxide − NirS, NirK
Nitrous oxide reduction − NosZ
Nitrogen fixation − NifH
Oxygenic Photosynthesis − PsaA, PsbA
Calvin−Benson cycle − RbcL
3−hydroxypropionate cycle − Mcr
4−hydroxybutyrate cycles − HbsC, HbsT
Reductive TCA cycle − AclB
Wood Ljungdahl pathway − CooS, AcsB
Agricultural − Switchgrass
Tropical Peatland
Dryland
Ecosystem
Log10 RPKM+1
4
3
2
1
0
Log10 TPM+1
4
3
2
1
0

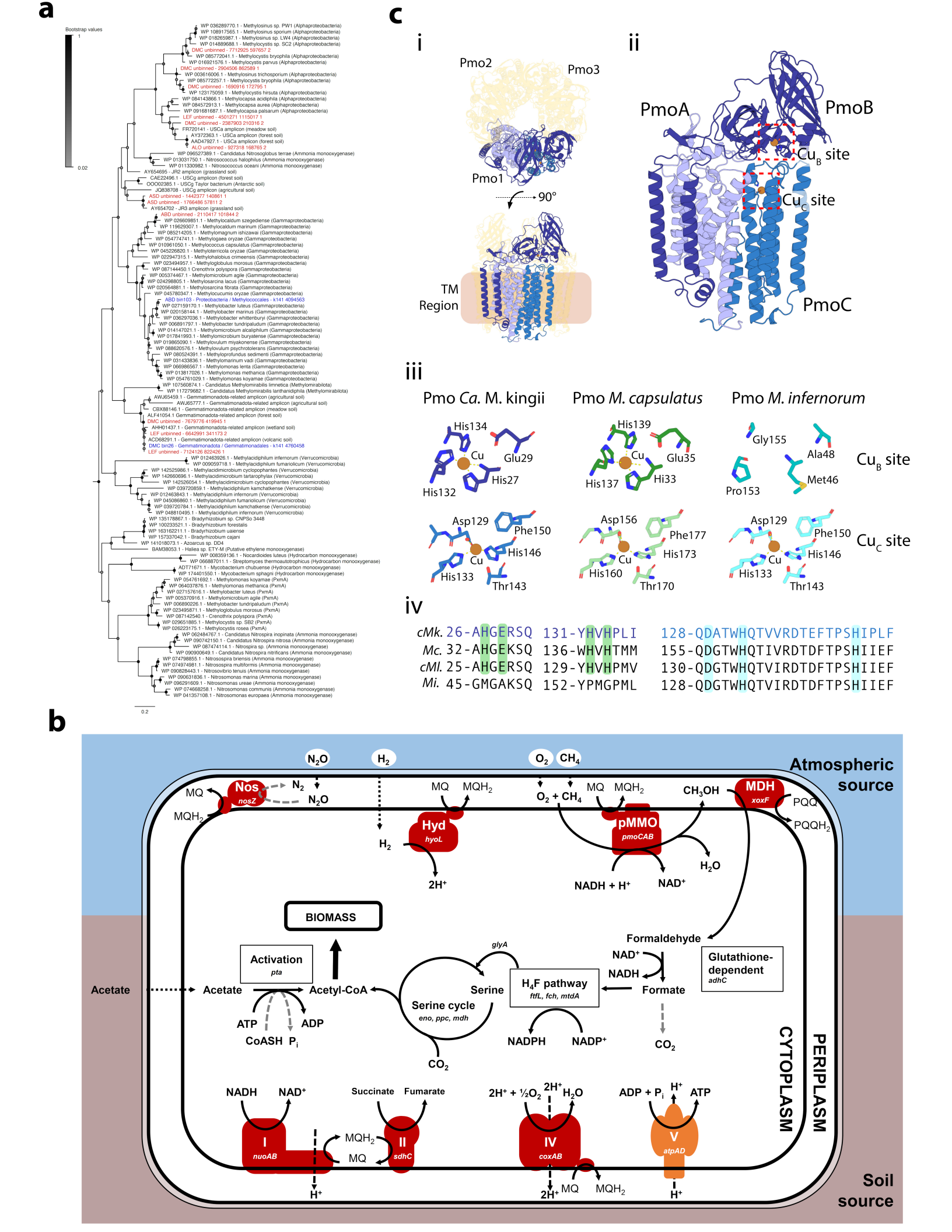
a
Bootstrap values
1
0.02
WP 036289770.1 - Methylosinus sp. PW1 (Alphaproteobacteria)
WP 108917565.1 - Methylosinus sporium (Alphaproteobacteria)
WP 018265987.1 - Methylosinus sp. LW4 (Alphaproteobacteria)
WP 014889688.1 - Methylocystis sp. SC2 (Alphaproteobacteria)
DMC unbinned - 7712925 597657 2
WP 085772041.1 - Methylocystis bryophila (Alphaproteobacteria)
WP 016921576.1 - Methylocystis parvus (Alphaproteobacteria)
DMC unbinned - 2904506 862589 1
WP 003616006.1 - Methylosinus trichosporium (Alphaproteobacteria)
WP 085772257.1 - Methylocystis bryophila (Alphaproteobacteria)
DMC unbinned - 1690916 172795 1
WP 123175059.1 - Methylocystis hirsuta (Alphaproteobacteria)
WP 084143866.1 - Methylocapsa aciditerrae (Alphaproteobacteria)
WP 084572913.1 - Methylocapsa aurea (Alphaproteobacteria)
WP 091681687.1 - Methylocapsa palsarum (Alphaproteobacteria)
LEF unbinned - 4501271 1115017 1
DMC unbinned - 2387903 210316 2
FR720141 - USCa amplicon (meadow soil)
AY372363.1 - USCa amplicon (forest soil)
AAD47927.1 - USCa amplicon (forest soil)
ALO unbinned - 927318 168765 2
WP 096527389.1 - Candidatus Nitrosoglobus terrae (Ammonia monooxygenase)
WP 013031750.1 - Nitrosococcus halophilus (Ammonia monooxygenase)
WP 011330982.1 - Nitrosococcus oceani (Ammonia monooxygenase)
AY654695 - JR2 amplicon (grassland soil)
CAE22496.1 - USCg amplicon (forest soil)
OOO02385.1 - USCg Taylor bacterium (Antarctic soil)
JQ838708 - USCg amplicon (agricultural soil)
ASD unbinned - 1442377 140861 1
ASD unbinned - 1766486 57811 2
AY654702 - JR3 amplicon (grassland soil)
ABD unbinned - 2110417 101844 2
WP 029609851.1 - Methylocaldum szegediense (Gammaproteobacteria)
WP 119629307.1 - Methylocaldum marinum (Gammaproteobacteria)
WP 085214205.1 - Methylomagnum ishizawai (Gammaproteobacteria)
WP 054774741.1 - Methylogaea oryzae (Gammaproteobacteria)
WP 010961050.1 - Methylococcus capsulatus (Gammaproteobacteria)
WP 045226820.1 - Methylobernicola oryzae (Gammaproteobacteria)
WP 022947315.1 - Methylohalobius crimeensis (Gammaproteobacteria)
WP 023494957.1 - Methyloglobulus morosus (Gammaproteobacteria)
WP 087144450.1 Crenothrix polyspora (Gammaproteobacteria)
WP 005374467.1 - Methylomicrobium agile (Gammaproteobacteria)
WP 024298805.1 - Methylosarcina lacus (Gammaproteobacteria)
WP 020564881.1 - Methylosarcina fibrata (Gammaproteobacteria)
WP 045780347.1 - Methylococcumis oryzae (Gammaproteobacteria)
ABD bin103 - Proteobacteria / Methylococcales - k141 4094563
WP 027159170.1 - Methylobacter luteus (Gammaproteobacteria)
WP 020158144.1 - Methylobacter marinus (Gammaproteobacteria)
WP 036297036.1 - Methylobacter whittenburyi (Gammaproteobacteria)
WP 006891797.1 - Methylobacter tundripaludum (Gammaproteobacteria)
WP 014147021.1 - Methylomicrobium alcaliphilum (Gammaproteobacteria)
WP 017841993.1 - Methylomicrobium buryatense (Gammaproteobacteria)
WP 019865090.1 - Methylovulum miyakonense (Gammaproteobacteria)
WP 088620576.1 - Methylovulum psychrotolerans (Gammaproteobacteria)
WP 080524391.1 - Methyloprofundus sedimenti (Gammaproteobacteria)
WP 031433836.1 - Methylomarinum vadi (Gammaproteobacteria)
WP 066986567.1 - Methylomonas lenta (Gammaproteobacteria)
WP 013817026.1 - Methylomonas methanica (Gammaproteobacteria)
WP 054761029.1 - Methylomonas koyamae (Gammaproteobacteria)
WP 107560874.1 - Candidatus Methylomirabilis limnetica (Methylomirabilota)
WP 117279682.1 - Candidatus Methylomirabilis lanthanidiphila (Methylomirabilota)
AWJ65459.1 - Gemmatimonadota-related amplicon (agricultural soil)
AWJ65777.1 - Gemmatimonadota-related amplicon (agricultural soil)
CBX88146.1 - Gemmatimonadota-related amplicon (meadow soil)
ALF41054.1 Gemmatimonadota-related amplicon (forest soil)
DMC unbinned - 7679776 419945 1
AHH01437.1 - Gemmatimonadota-related amplicon (wetland soil)
LEF unbinned - 6642991 341173 2
ACD68291.1 - Gemmatimonadota-related amplicon (volcanic soil)
DMC bin26 - Gemmatimonadota / Gemmatimonadales - k141 4760458
LEF unbinned - 7124126 822426 1
WP 012463926.1 - Methylacidiphilum infernorum (Verrucomicrobia)
WP 009059718.1 - Methylacidiphilum fumariolicum (Verrucomicrobia)
WP 142525986.1 - Methylacidimicrobium cyclopophantes (Verrucomicrobia)
WP 142660696.1 - Methylacidimicrobium tartarophylax (Verrucomicrobia)
WP 142526054.1 - Methylacidimicrobium cyclopophantes (Verrucomicrobia)
WP 039720859.1 - Methylacidiphilum kamchatkense (Verrucomicrobia)
WP 012463843.1 - Methylacidiphilum infernorum (Verrucomicrobia)
WP 045086860.1 - Methylacidiphilum fumariolicum (Verrucomicrobia)
WP 039720784.1 - Methylacidiphilum kamchatkense (Verrucomicrobia)
WP 048810495.1 - Methylacidiphilum infernorum (Verrucomicrobia)
WP 135178867.1 - Bradyrhizobium sp. CNPSo 3448
WP 100233521.1 - Bradyrhizobium forestalis
WP 163162211.1 - Bradyrhizobium uaiense
WP 157337042.1 - Bradyrhizobium cajani
WP 141018073.1 - Azoarcus sp. DD4
BAM38053.1 - Haliea sp. ETY-M (Putative ethylene monooxygenase)
WP 008359136.1 - Nocardioides luteus (Hydrocarbon monooxygenase)
WP 066887011.1 - Streptomyces thermoautotrophicus (Hydrocarbon monooxygenase)
ADT71671.1 - Mycobacterium chubuense (Hydrocarbon monooxygenase)
WP 174401550.1 - Mycobacterium sphagni (Hydrocarbon monooxygenase)
WP 054761692.1 - Methylomonas koyamae (PxmA)
WP 064037876.1 - Methylomonas methanica (PxmA)
WP 027157616.1 - Methylobacter luteus (PxmA)
WP 005370916.1 - Methylomicrobium agile (PxmA)
WP 066890226.1 - Methylobacter tundripaludum (PxmA)
WP 023495871.1 - Methyloglobulus morosus (PxmA)
WP 087142540.1 - Crenothrix polyspora (PxmA)
WP 029651885.1 - Methylocystis sp. SB2 (PxmA)
WP 026223175.1 - Methylocystis rosea (PxmA)
WP 062484767.1 - Candidatus Nitrospira inopinata (Ammonia monooxygenase)
WP 090742150.1 - Candidatus Nitrospira nitrosa (Ammonia monooxygenase)
WP 087474114.1 - Nitrospira sp. (Ammonia monooxygenase)
WP 090900649.1 - Candidatus Nitrospira nitricans (Ammonia monooxygenase)
WP 074798855.1 - Nitrosospira briensis (Ammonia monooxygenase)
WP 074974981.1 - Nitrosospira multiformis (Ammonia monooxygenase)
WP 090828443.1 - Nitrosovibrio tenuis (Ammonia monooxygenase)
WP 090631836.1 - Nitrosomonas marina (Ammonia monooxygenase)
WP 096291609.1 - Nitrosomonas ureae (Ammonia monooxygenase)
WP 074668258.1 - Nitrosomonas communis (Ammonia monooxygenase)
WP 041357108.1 - Nitrosomonas europaea (Ammonia monooxygenase)
0.2
c
i
Pmo2
Pmo3
Pmo1
90°
TM Region
ii
PmoA
PmoB
Cu$_B$ site
Cu$_C$ site
PmoC
iii
Pmo Ca. M. kingii
Pmo M. capsulatus
Pmo M. infernorum
His134
Cu
Glu29
His27
His132
His139
Glu35
His137
Hi33
Gly155
Ala48
Met46
Pro153
Cu$_B$ site
Asp129
Phe150
His146
Thr143
Asp156
Phe177
His173
His160
Thr170
Cu$_C$ site
iv
cMk. 26-AHGERSQ 131-YHVHPLI 128-QDATWHQTVVRDTEFTPSHIPLF
Mc. 32-AHGEKSQ 136-WHVHTMM 155-QDGTWHQTIVRDTDFTPSHIIEF
cMl. 25-AHGERSQ 129-YHVHPMV 130-QDGTWHQTVIRDTDFTPSHIIEF
Mi. 45-GMGAKSQ 152-YPMGPML 128-QDGTWHQTVIRDTDFTPSHIIEF
b
Atmospheric source
Soil source
CYTOPLASM
PERIPLASM
N2O
H2
O2
CH4
Nos
nosZ
N2
MQ
MQH2
Hyd
hyoL
2H+
O2 + CH4
pMMO
pmoCAB
H2O
NADH + H+
NAD+
CH3OH
MDH
xoxF
PQQ
PQQH2
BIOMASS
Activation
pta
Acetate
Acetyl-CoA
ATP
ADP
CoASH
Pi
Serine cycle
eno, ppc, mdh
glyA
Serine
H4F pathway
ftfL, fch, mtdA
NADPH
NADP+
CO2
Formaldehyde
NAD+
NADH
Formate
Glutathione-dependent
adhC
NADH
Succinate
Fumarate
I
nuoAB
II
sdhC
IV
coxAB
V
atpAD
2H+ + ½O2
ADP + Pi
H+

a

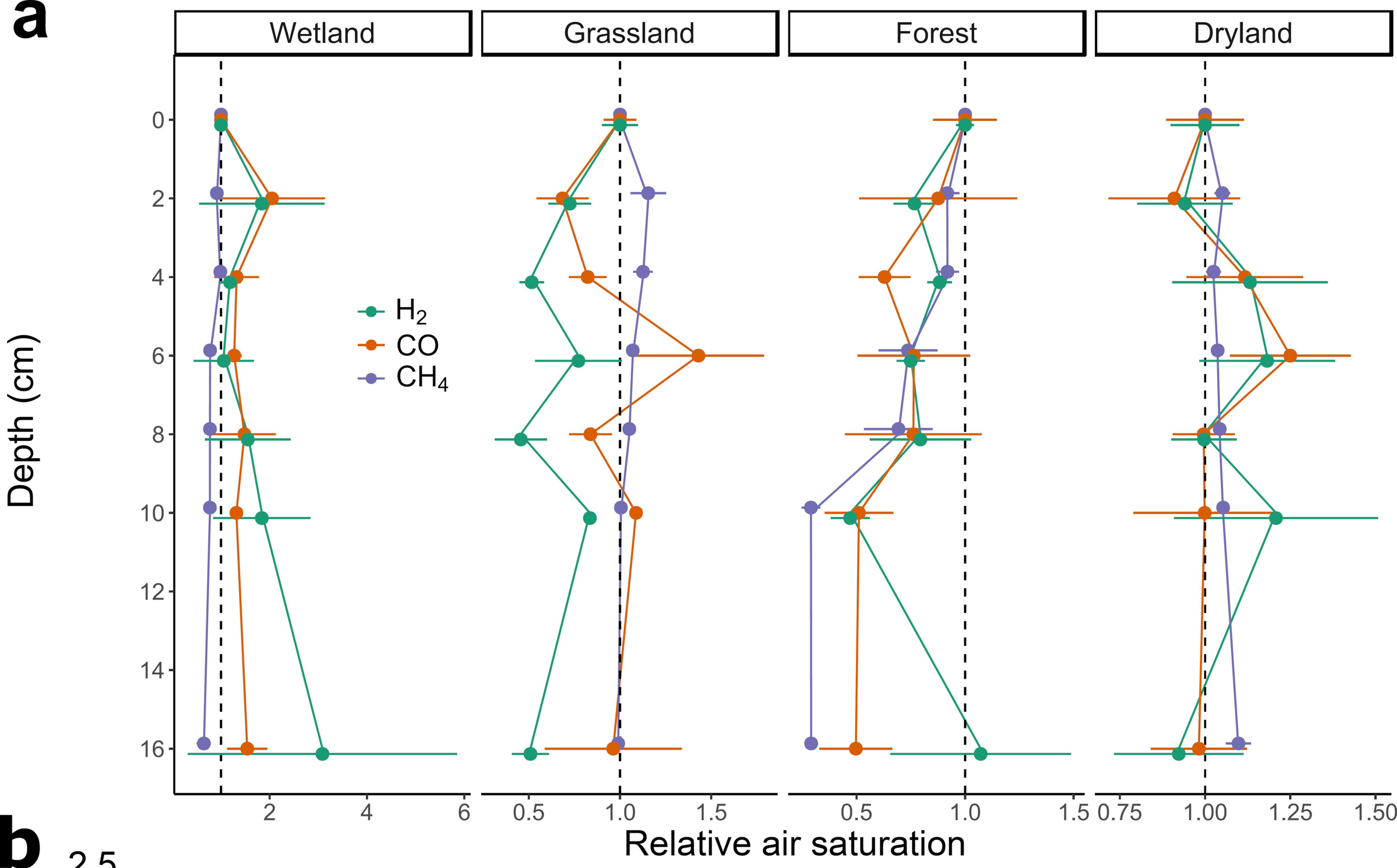
Wetland
Grassland
Forest
Dryland
Depth (cm)
0
2
4
6
8
10
12
14
16
H_2
CO
CH_4
2
4
6
0.5
1.0
1.5
0.5
1.0
1.5
0.75
1.00
1.25
1.50
Relative air saturation

b

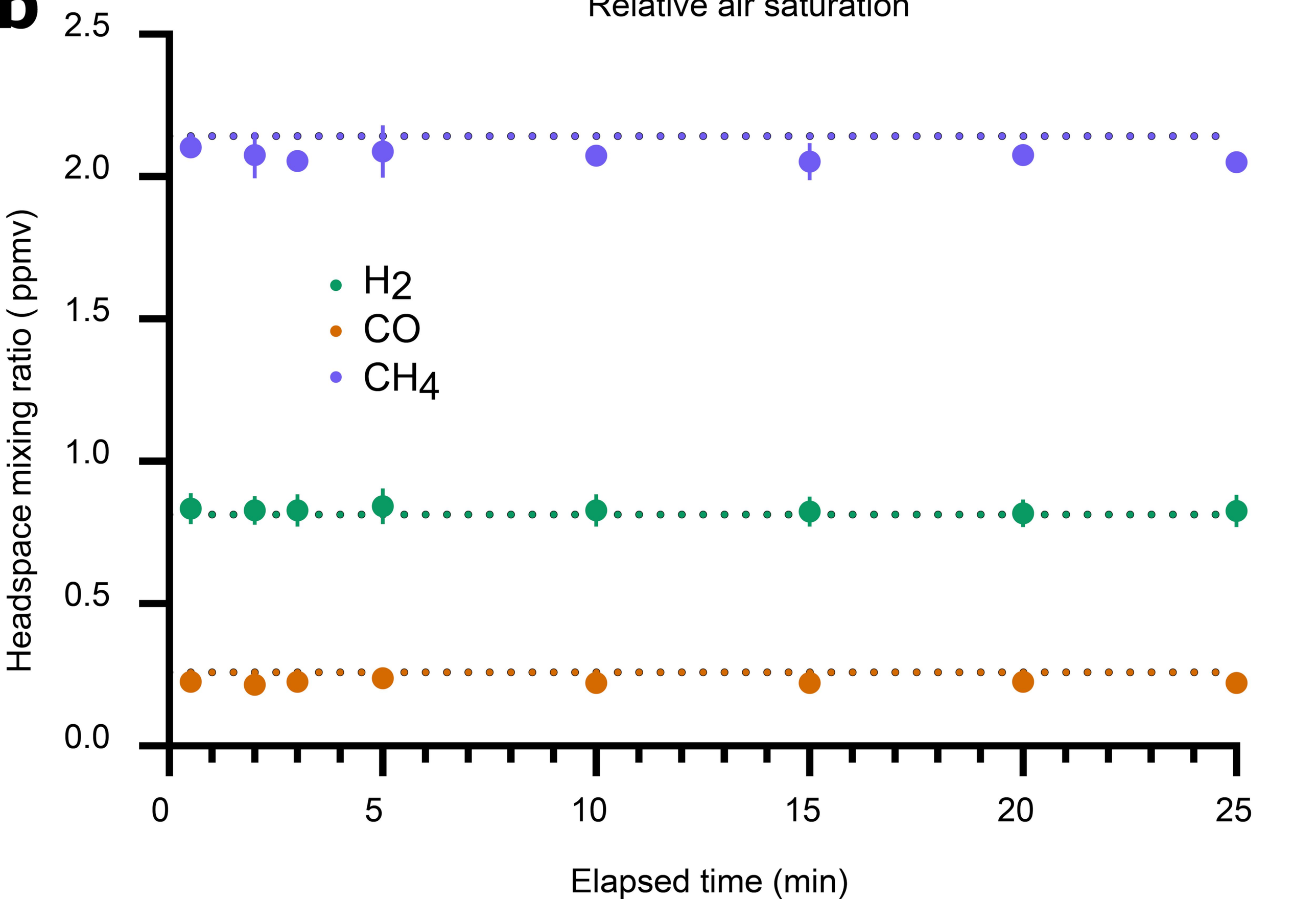
Headspace mixing ratio (ppmv)
2.5
2.0
1.5
1.0
0.5
0.0
H_2
CO
CH_4
0
5
10
15
20
25
Elapsed time (min)

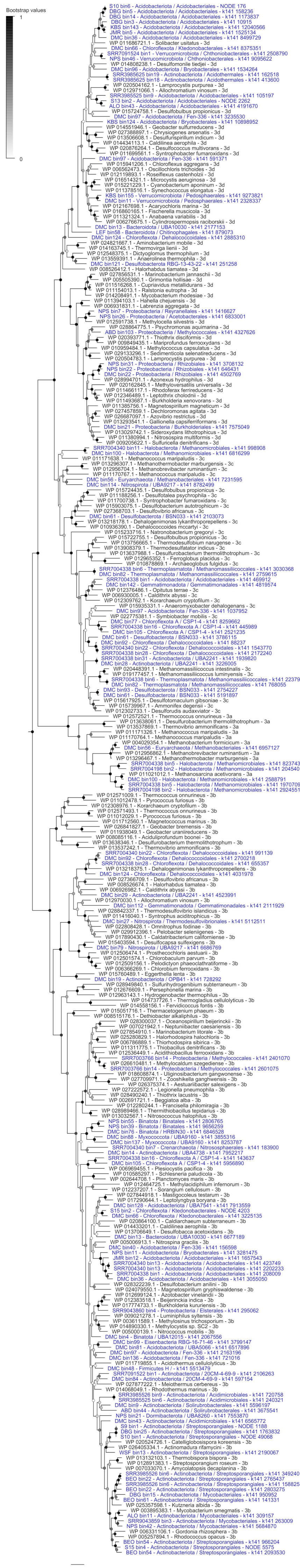
Bootstrap values
1
0
S10 bin6 - Acidobacteriota / Acidobacteriales - NODE 176
DBG bin5 - Acidobacteriota / Acidobacteriales - k141 158236
DBG bin14 - Acidobacteriota / Acidobacteriales - k141 1173837
DBG bin3 - Acidobacteriota / Acidobacteriales - k141 10915
KBS bin143 - Acidobacteriota / Acidobacteriales - k141 12040566
JMR bin5 - Acidobacteriota / Acidobacteriales - k141 1525134
DMC bin36 - Acidobacteriota / Acidobacteriales - k141 8499729
WP 011686721.1 - Solibacter usitatus - 3d
DMC bin66 - Chloroflexota / Ktedonobacterales - k141 8375351
SRR7091524 bin1 - Verrucomicrobiota / Chthoniobacterales - k141 2508790
NPS bin46 - Verrucomicrobiota / Chthoniobacterales - k141 9095622
WP 014808238.1 - Desulfomonile tiedjei - 3d
DMC bin96 - Acidobacteriota / Bryobacterales - k141 1534264
SRR3985625 bin19 - Actinobacteriota / Acidothermales - k141 162518
SRR3985625 bin18 - Actinobacteriota / Acidothermales - k141 413600
WP 020504162.1 - Lamprocystis purpurea - 3d
WP 012971066.1 - Allochromatium vinosum - 3d
SRR3985525 bin9 - Acidobacteriota / Acidobacteriales - k141 105197
S13 bin2 - Acidobacteriota / Acidobacteriales - NODE 2262
ALO bin43 - Acidobacteriota / Acidobacteriales - k141 4191670
WP 015724758.1 - Desulfobulbus propionicus - 3d
DMC bin97 - Acidobacteriota / Fen-336 - k141 3235530
KBS bin124 - Acidobacteriota / Bryobacterales - k141 10898952
WP 014551946.1 - Geobacter sulfurreducens - 3d
WP 027388897.1 - Chrysiogenes arsenatis - 3d
WP 013506608.1 - Desulfurispirillum indicum - 3d
WP 014434113.1 - Caldilinea aerophila - 3d
WP 020876264.1 - Desulfococcus multivorans - 3d
WP 011699561.1 - Syntrophobacter fumaroxidans - 3d
DMC bin97 - Acidobacteriota / Fen-336 - k141 591371
WP 015941206.1 - Chloroflexus aggregans - 3d
WP 006562473.1 - Oscillochloris trichoides - 3d
WP 012119893.1 - Roseiflexus castenholzii - 3d
WP 016514321.1 - Microcystis aeruginosa - 3d
WP 015221229.1 - Cyanobacterium aponinum - 3d
WP 011378516.1 - Synechococcus elongatus - 3d
KBS bin155 - Verrucomicrobiota / Pedosphaerales - k141 9273821
DMC bin11 - Verrucomicrobiota / Pedosphaerales - k141 2328337
WP 012167698.1 - Acaryochloris marina - 3d
WP 016860165.1 - Fischerella muscicola - 3d
WP 011321324.1 - Anabaena variabilis - 3d
WP 006276675.1 - Cylindrospermopsis raciborskii - 3d
DMC bin13 - Bacteroidota / UBA10030 - k141 2177153
LEF bin58 - Bacteroidota / Chitinophagales - k141 879073
DMC bin124 - Chloroflexota / Dehalococcoidales - k141 2885310
WP 024821667.1 - Aminobacterium mobile - 3d
WP 014163745.1 - Thermovirga lienii - 3d
WP 012548375.1 - Dictyoglomus thermophilum - 3d
WP 013559391.1 - Anaerolinea thermophila - 3d
DMC bin121 - Desulfobacterota RBG-13-43-22 - k141 251258
WP 008526412.1 - Halorhabdus tiamatea - 3d
WP 027856531.1 - Marinobacterium jannaschii - 3d
WP 005505390.1 - Grimontia hollisae - 3d
WP 011516268.1 - Cupriavidus metallidurans - 3d
WP 011154013.1 - Ralstonia eutropha - 3d
WP 014208491.1 - Mycobacterium rhodesiae - 3d
WP 011394103.1 - Hahella chejuensis - 3d
WP 006931831.1 - Labrenzia aggregata - 3d
NPS bin7 - Proteobacteria / Reyranellales - k141 1416627
NPS bin26 - Proteobacteria / Acetobacterales - k141 6833001
WP 012591738.1 - Methylocella silvestris - 3d
WP 028864775.1 - Psychromonas aquimarina - 3d
ABD bin103 - Proteobacteria / Methylococcales - k141 4327626
WP 020393771.1 - Thiothrix disciformis - 3d
WP 009849435.1 - Mariprofundus ferrooxydans - 3d
WP 010959484.1 - Methylococcus capsulatus - 3d
WP 029133296.1 - Sedimenticola selenatireducens - 3d
WP 020504783.1 - Lamprocystis purpurea - 3d
NPS bin31 - Proteobacteria / Rhizobiales - k141 3708132
NPS bin22 - Proteobacteria / Rhizobiales - k141 646431
DMC bin22 - Proteobacteria / Rhizobiales - k141 4502769
WP 028994701.1 - Azonexus hydrophilus - 3d
WP 020162845.1 - Methyloversatilis universalis - 3d
WP 011466117.1 - Rhodoferax ferrireducens - 3d
WP 012346489.1 - Leptothrix cholodnii - 3d
WP 011493687.1 - Burkholderia xenovorans - 3d
WP 011385756.1 - Magnetospirillum magneticum - 3d
WP 027457859.1 - Dechloromonas agitata - 3d
WP 026687097.1 - Azovibrio restrictus - 3d
WP 013293541.1 - Gallionella capsiferriformans - 3d
DMC bin21 - Proteobacteria / Burkholderiales - k141 7575049
WP 013029742.1 - Sideroxydans lithotrophicus - 3d
WP 011380994.1 - Nitrosospira multiformis - 3d
WP 009205622.1 - Sulfuricella denitrificans - 3d
SRR7004340 bin11 - Halobacterota / Methanomicrobiales - k141 998908
DMC bin100 - Halobacterota / Methanomicrobiales - k141 6816299
WP 011171638.1 - Methanococcus maripaludis - 3c
WP 013296307.1 - Methanothermobacter marburgensis - 3c
WP 012956704.1 - Methanobrevibacter ruminantium - 3c
WP 011170767.1 - Methanococcus maripaludis - 3c
DMC bin56 - Euryarchaeota / Methanobacteriales - k141 7231595
DMC bin114 - Nitrospirota / UBA9217 - k141 8782499
WP 015724435.1 - Desulfobulbus propionicus - 3c
WP 011188256.1 - Desulfotalea psychrophila - 3c
WP 011700738.1 - Syntrophobacter fumaroxidans - 3c
WP 015903075.1 - Desulfobacterium autotrophicum - 3c
WP 027368703.1 - Desulfovibrio africanus - 3c
DMC bin61 - Desulfobacterota / BSN033 - k141 2103073
WP 013218178.1 - Dehalogenimonas lykanthroporepellens - 3c
WP 010936390.1 - Dehalococcoides mccartyi - 3c
WP 015233716.1 - Natronobacterium gregoryi - 3c
WP 015722755.1 - Desulfobulbus propionicus - 3c
WP 013756665.1 - Thermodesulfobium narugense - 3c
WP 013908379.1 - Thermodesulfatator indicus - 3c
WP 013637988.1 - Desulfurobacterium thermolithotrophum - 3c
WP 012965352.1 - Ferroglobus placidus - 3c
WP 010878869.1 - Archaeoglobus fulgidus - 3c
SRR7004338 bin6 - Thermoplasmatota / Methanomassiliicoccales - k141 3030368
DMC bin82 - Thermoplasmatota / Methanomassiliicoccales - k141 2759615
SRR7004338 bin1 - Acidobacteriota / Acidobacteriales - k141 469912
DMC bin142 - Gemmatimonadota / Gemmatimonadales - k141 4819574
WP 012376486.1 - Opitutus terrae - 3c
WP 006930005.1 - Caldithrix abyssi - 3c
WP 012309762.1 - Korarchaeum cryptofilum - 3c
WP 015935331.1 - Anaeromyxobacter dehalogenans - 3c
DMC bin97 - Acidobacteriota / Fen-336 - k141 1037952
WP 022775381.1 - Symbiobacter mobilis - 3c
DMC bin77 - Chloroflexota A / CSP1-4 - k141 8259662
SRR7004338 bin16 - Chloroflexota A / CSP1-4 - k141 445989
DMC bin105 - Chloroflexota A / CSP1-4 - k141 2521235
DMC bin61 - Desulfobacterota / BSN033 - k141 3786115
DMC bin92 - Chloroflexota / Dehalococcoidales - k141 88237
SRR7004340 bin22 - Chloroflexota / Dehalococcoidales - k141 1543770
SRR7004338 bin28 - Chloroflexota / Dehalococcoidales - k141 2172240
SRR7004338 bin31 - Actinobacteriota / UBA2241 - k141 1939820
DMC bin28 - Actinobacteriota / UBA2241 - k141 3226005
WP 020448391.1 - Methanomassiliicoccus intestinalis - 3c
WP 019177457.1 - Methanomassiliicoccus luminyensis - 3c
SRR7004338 bin6 - Thermoplasmatota / Methanomassiliicoccales - k141 2237998
DMC bin82 - Thermoplasmatota / Methanomassiliicoccales - k141 768055
DMC bin93 - Desulfobacterota / BSN033 - k141 2754227
DMC bin61 - Desulfobacterota / BSN033 - k141 5191897
WP 015617925.1 - Desulfotomaculum gibsoniae - 3c
WP 015739967.1 - Ammonifex degensii - 3c
WP 012302733.1 - Desulforudis audaxviator - 3c
WP 012572521.1 - Thermococcus onnurineus - 3a
WP 013638061.1 - Desulfurobacterium thermolithotrophum - 3a
WP 013537869.1 - Thermovibrio ammonificans - 3a
WP 011171326.1 - Methanococcus maripaludis - 3a
WP 011170764.1 - Methanococcus maripaludis - 3a
WP 004029354.1 - Methanobacterium formicicum - 3a
DMC bin56 - Euryarchaeota / Methanobacteriales - k141 6957127
WP 012956862.1 - Methanobrevibacter ruminantium - 3a
WP 013296467.1 - Methanothermobacter marburgensis - 3a
SRR7004338 bin5 - Halobacterota / Methanomicrobiales - k141 823743
SRR7004198 bin2 - Halobacterota / Methanomicrobiales - k141 204540
WP 011021012.1 - Methanosarcina acetivorans - 3a
DMC bin100 - Halobacterota / Methanomicrobiales - k141 2588791
SRR7004338 bin5 - Halobacterota / Methanomicrobiales - k141 1970709
SRR7004198 bin2 - Halobacterota / Methanomicrobiales - k141 2924551
WP 012571009.1 - Thermococcus onnurineus - 3b
WP 011012478.1 - Pyrococcus furiosus - 3b
WP 012308976.1 - Korarchaeum cryptofilum - 3b
WP 012571493.1 - Thermococcus onnurineus - 3b
WP 011012029.1 - Pyrococcus furiosus - 3b
WP 011712560.1 - Magnetococcus marinus - 3b
WP 026841827.1 - Geobacter bremensis - 3b
WP 011938049.1 - Geobacter uraniireducens - 3b
WP 008085116.1 - Aciduliprofundum boonei - 3b
WP 013638346.1 - Desulfurobacterium thermolithotrophum - 3b
WP 013537242.1 - Thermovibrio ammonificans - 3b
SRR7004340 bin22 - Chloroflexota / Dehalococcoidales - k141 991139
DMC bin92 - Chloroflexota / Dehalococcoidales - k141 2700218
SRR7004338 bin28 - Chloroflexota / Dehalococcoidales - k141 655357
WP 013218375.1 - Dehalogenimonas lykanthroporepellens - 3b
DMC bin124 - Chloroflexota / Dehalococcoidales - k141 4031978
WP 027366709.1 - Desulfovibrio africanus - 3b
WP 008526674.1 - Halorhabdus tiamatea - 3b
WP 006926982.1 - Caldithrix abyssi - 3b
DMC bin29 - Actinobacteriota / UBA2241 - k141 4523991
WP 012970030.1 - Allochromatium vinosum - 3b
DMC bin112 - Gemmatimonadota / Gemmatimonadales - k141 2111929
WP 028842337.1 - Thermodesulfovibrio islandicus - 3b
WP 011416040.1 - Syntrophus aciditrophicus - 3b
DMC bin27 - Nitrospirota / Thermodesulfovibrionales - k141 5112511
WP 022808428.1 - Omnitrophus fodinae - 3b
WP 029912396.1 - Pelobacter seleniigenes - 3b
WP 017890430.1 - Caldatribacterium californiense - 3b
WP 015403594.1 - Desulfocapsa sulfexigens - 3b
DMC bin79 - Nitrospirota / UBA9217 - k141 6686769
WP 012506474.1 - Prosthecochloris aestuarii - 3b
WP 012501574.1 - Chlorobaculum parvum - 3b
WP 012509156.1 - Pelodictyon phaeoclathratiforme - 3b
WP 006366269.1 - Chlorobium ferrooxidans - 3b
WP 015760489.1 - Eggerthella lenta - 3b
DMC bin19 - Actinobacteriota / OPB41 - k141 728292
WP 028949840.1 - Sulfurihydrogenibium subterraneum - 3b
WP 012676609.1 - Persephonella marina - 3b
WP 012963143.1 - Hydrogenobacter thermophilus - 3b
WP 014737726.1 - Thermogladius cellulolyticus - 3b
WP 014558156.1 - Fervidicoccus fontis - 3b
WP 015051716.1 - Thermacetogenium phaeum - 3b
WP 008515176.1 - Dethiobacter alkaliphilus - 3b
WP 028300037.1 - Oceanospirillum beijerinckii - 3b
WP 007021942.1 - Neptuniibacter caesariensis - 3b
WP 027854910.1 - Marinobacterium litorale - 3b
WP 025280829.1 - Halorhodospira halochloris - 3b
WP 006786889.1 - Thiorhodospira sibirica - 3b
WP 011311775.1 - Thiobacillus denitrificans - 3b
WP 012536449.1 - Acidithiobacillus ferrooxidans - 3b
SRR7003766 bin14 - Proteobacteria / Methylococcales - k141 2401070
WP 026610481.1 - Methylocaldum szegediense - 3b
SRR7003766 bin14 - Proteobacteria / Methylococcales - k141 2601075
WP 018608874.1 - Uliginosibacterium gangwonense - 3b
WP 027709971.1 - Zooshikella ganghwensis - 3b
WP 026375374.1 - Aestuariibacter salexigens - 3b
WP 027222572.1 - Legionella pneumophila - 3b
WP 028490240.1 - Thiothrix lacustris - 3b
WP 002691721.1 - Beggiatoa alba - 3b
WP 012280244.1 - Francisella philomiragia - 3b
WP 028989466.1 - Thermithiobacillus tepidarius - 3b
WP 013032567.1 - Nitrosococcus halophilus - 3b
NPS bin55 - Binatota / Binatales - k141 2806765
NPS bin39 - Binatota / Binatales - k141 9656259
DMC bin76 - Binatota / HRBIN30 - k141 6846528
DMC bin88 - Myxococcota / UBA9160 - k141 3855316
DMC bin137 - Myxococcota / UBA9160 - k141 8253787
SRR7004340 bin7 - Crenarchaeota / Nitrososphaerales - k141 183900
DMC bin14 - Actinobacteriota / UBA4738 - k141 7952217
SRR7004338 bin16 - Chloroflexota A / CSP1-4 - k141 143637
DMC bin105 - Chloroflexota A / CSP1-4 - k141 5956890
WP 006969455.1 - Plesiocystis pacifica - 3b
WP 010585297.1 - Schlesneria paludicola - 3b
WP 002644708.1 - Planctomyces maris - 3b
WP 012464725.1 - Methylacidiphilum infernorum - 3b
WP 012237207.1 - Sorangium cellulosum - 3b
WP 027844918.1 - Mastigocoleus testarum - 3b
WP 017290644.1 - Leptolyngbya boryana - 3b
DMC bin128 - Acidobacteriota / UBA7541 - k141 7913559
S15 bin2 - Chloroflexota / Ktedonobacterales - NODE 4203
DMC bin66 - Chloroflexota / Ktedonobacterales - k141 3225135
WP 020864100.1 - Caldiarchaeum subterraneum - 3b
WP 014433201.1 - Caldilinea aerophila - 3b
WP 013706649.1 - Desulfobacca acetoxidans - 3b
DMC bin13 - Bacteroidota / UBA10030 - k141 6677189
WP 005006913.1 - Nitrospina gracilis - 3b
DMC bin40 - Acidobacteriota / Fen-336 - k141 156598
NPS bin11 - Acidobacteriota / Bryobacterales - k141 3281475
JMR bin12 - Acidobacteriota / Acidobacteriales - k141 1657543
SRR7004340 bin13 - Acidobacteriota / Acidobacteriales - k141 423749
SRR7004340 bin13 - Acidobacteriota / Acidobacteriales - k141 2202233
SRR7004338 bin1 - Acidobacteriota / Acidobacteriales - k141 208009
DMC bin36 - Acidobacteriota / Acidobacteriales - k141 3055050
WP 028322239.1 - Desulfobacterium anilini - 3b
WP 024079550.1 - Magnetospirillum gryphiswaldense - 3b
WP 012699124.1 - Azotobacter vinelandii - 3b
WP 012383518.1 - Beijerinckia indica - 3b
WP 017774733.1 - Burkholderia kururiensis - 3b
SRR9043860 bin4 - Proteobacteria / Elsterales - k141 295062
WP 009021278.1 - Luminiphilus syltensis - 3b
WP 003611589.1 - Methylosinus trichosporium - 3b
WP 014890330.1 - Methylocystis sp. SC2 - 3b
WP 005000139.1 - Nitrococcus mobilis - 3b
DMC bin4 - Binatota / UBA12015 - k141 2067556
DMC bin99 - Eisenbacteria RBG-16-71-46 - k141 3799147
DMC bin81 - Acidobacteriota / UBA5066 - k141 6517896
DMC bin97 - Acidobacteriota / Fen-336 - k141 2163196
DMC bin136 - Acidobacteriota / Fen-336 - k141 721016
WP 011719855.1 - Acidothermus cellulolyticus - 3b
DMC bin48 - Firmicutes H / - k141 5513479
SRR7091522 bin1 - Actinobacteriota / 20CM-4-69-9 - k141 2106263
DMC bin84 - Actinobacteriota / 20CM-4-69-9 - k141 597154
WP 027877222.1 - Meiothermus cerbereus - 3b
WP 014068049.1 - Rhodothermus marinus - 3b
SRR3985526 bin9 - Actinobacteriota / Acidimicrobiales - k141 720758
SRR3985525 bin6 - Actinobacteriota / Acidimicrobiales - k141 240321
DMC bin9 - Actinobacteriota / Solirubrobacterales - k141 5596197
ABD bin44 - Actinobacteriota / Solirubrobacterales - k141 3675541
NPS bin21 - Dormibacterota / UBA8260 - k141 7553870
DMC bin43 - Actinobacteriota / Acidimicrobiales - k141 6565772
S9 bin1 - Actinobacteriota / Streptosporangiales - NODE 1188
DBG bin25 - Actinobacteriota / Streptosporangiales - k141 1763832
S10 bin1 - Actinobacteriota / Streptosporangiales - NODE 49068
WP 020524726.1 - Catelliglobosispora koreensis - 3b
WP 026405334.1 - Actinomadura rifamycini - 3b
WSF bin13 - Actinobacteriota / Streptosporangiales - k141 2190067
WP 013132103.1 - Thermobispora bispora - 3b
WP 012891383.1 - Streptosporangium roseum - 3b
WP 007033070.1 - Amycolatopsis decaplanina - 3b
SRR3985526 bin6 - Actinobacteriota / Streptosporangiales - k141 349240
BEO bin22 - Actinobacteriota / Streptosporangiales - k141 2765437
SRR3985526 bin6 - Actinobacteriota / Streptosporangiales - k141 158825
BEO bin22 - Actinobacteriota / Streptosporangiales - k141 2803275
DBG bin15 - Actinobacteriota / Mycobacteriales - k141 950952
BEO bin61 - Actinobacteriota / Streptosporangiales - k141 141331
WP 025357598.1 - Kutzneria albida - 3b
WP 003895383.1 - Mycobacterium smegmatis - 3b
ALO bin11 - Actinobacteriota / Mycobacteriales - k141 309157
SRR9043859 bin3 - Actinobacteriota / Mycobacteriales - k141 263009
NPS bin42 - Actinobacteriota / Mycobacteriales - k141 5684870
WP 006331106.1 - Gordonia rhizosphera - 3b
WP 005257894.1 - Rhodococcus opacus - 3b
BEO bin54 - Actinobacteriota / Streptosporangiales - k141 966204
S15 bin4 - Actinobacteriota / Streptosporangiales - NODE 5575
BEO bin54 - Actinobacteriota / Streptosporangiales - k141 2093530
0.3

a

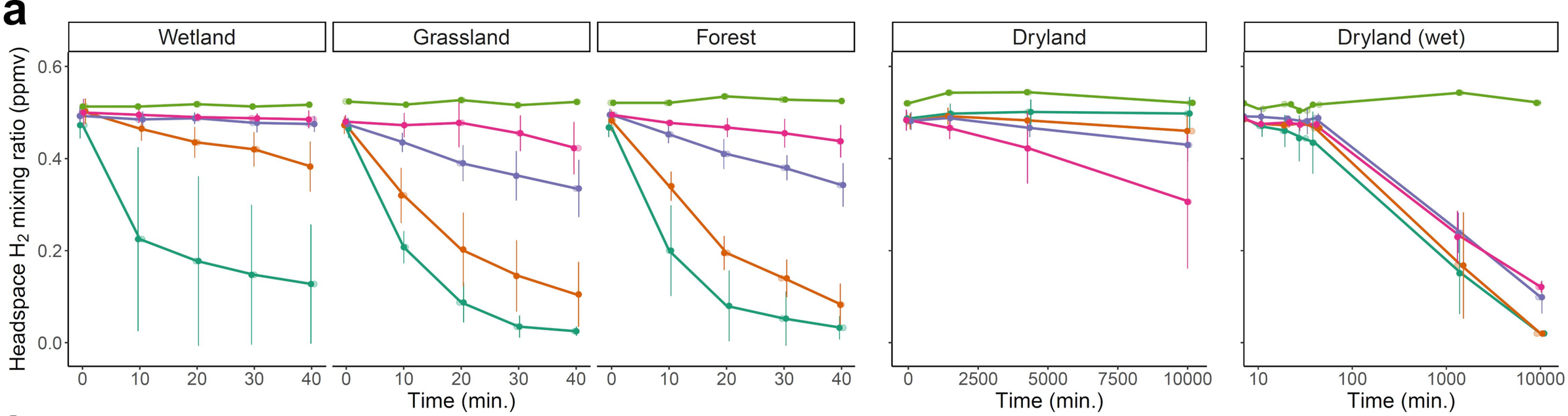
Wetland
Grassland
Forest
Dryland
Dryland (wet)
Headspace H_2 mixing ratio (ppmv)
0.0
0.2
0.4
0.6
0 10 20 30 40
0 2500 5000 7500 10000
10 100 1000 10000
Time (min.)

b

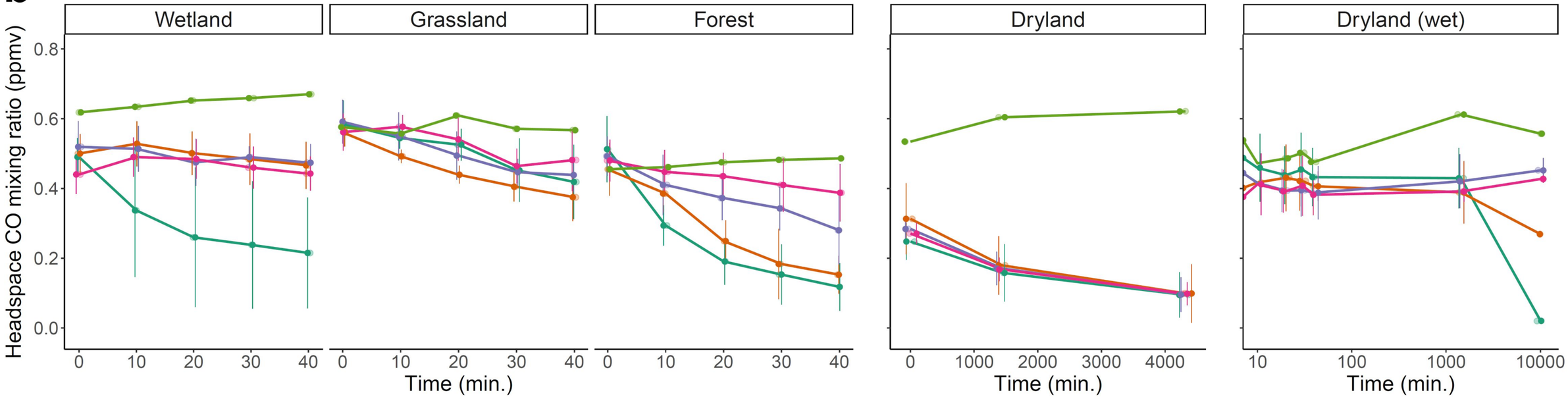
Wetland
Grassland
Forest
Dryland
Dryland (wet)
Headspace CO mixing ratio (ppmv)
0.0
0.2
0.4
0.6
0.8
0 10 20 30 40
0 1000 2000 3000 4000
10 100 1000 10000
Time (min.)
Depth (cm)
0–5
5–10
15–20
25–30
Control

c

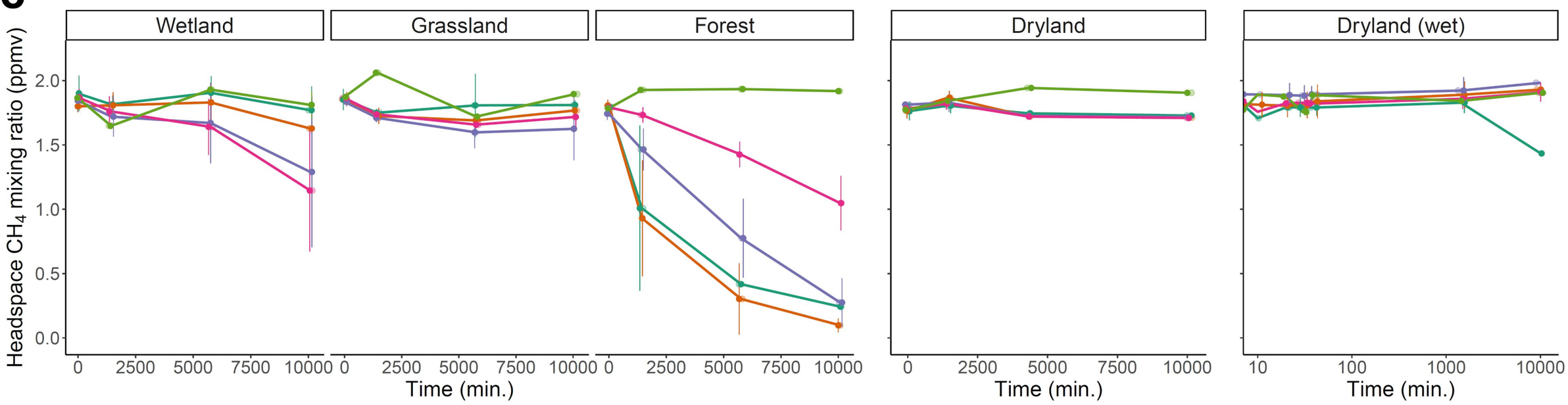
Wetland
Grassland
Forest
Dryland
Dryland (wet)
Headspace CH_4 mixing ratio (ppmv)
0.0
0.5
1.0
1.5
2.0
0 2500 5000 7500 10000
10 100 1000 10000
Time (min.)

d

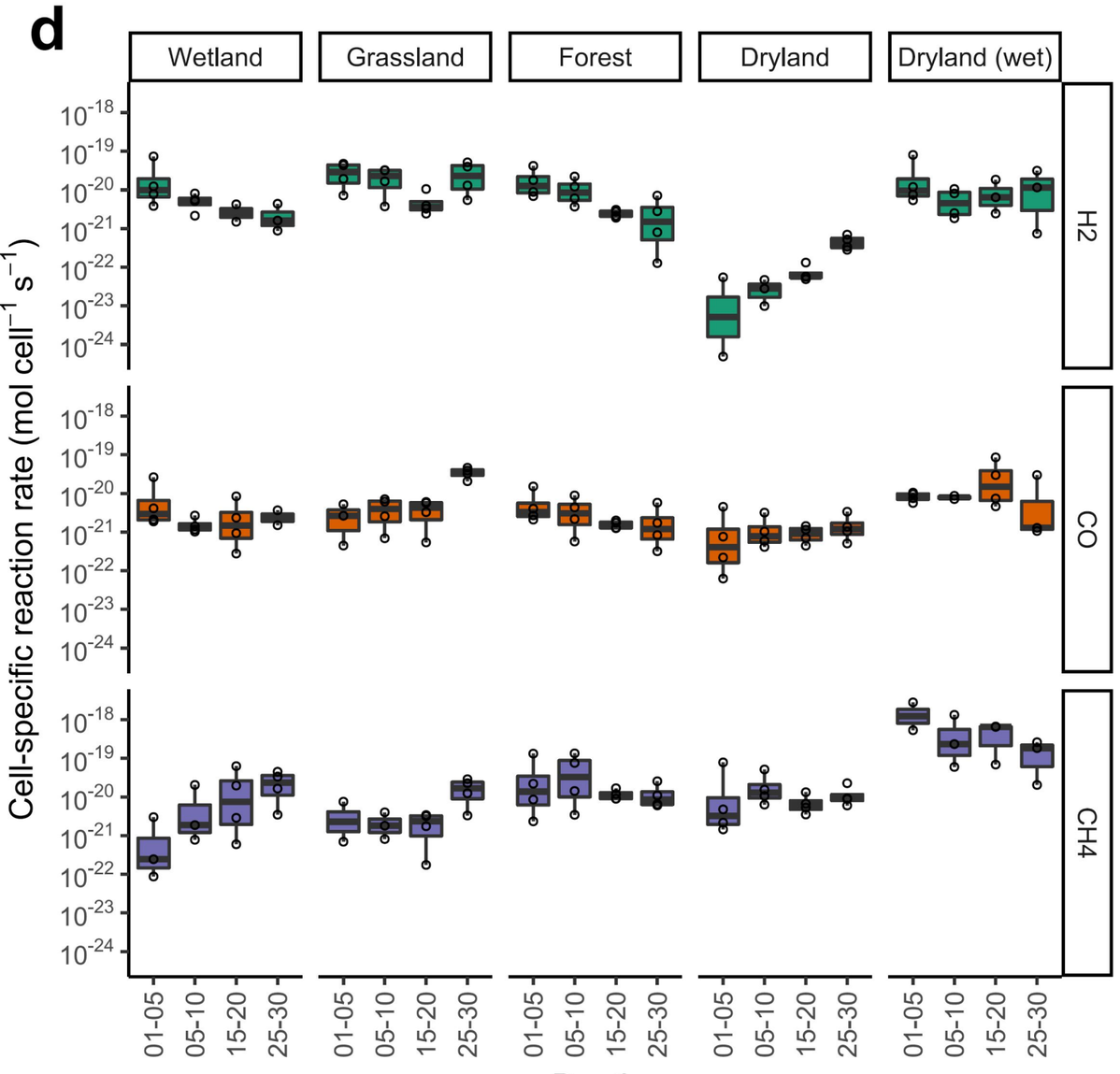
Wetland
Grassland
Forest
Dryland
Dryland (wet)
H2
CO
CH4
Cell-specific reaction rate (mol cell^{-1} s^{-1})
10^{-18}
10^{-19}
10^{-20}
10^{-21}
10^{-22}
10^{-23}
10^{-24}
01-05
05-10
15-20
25-30
Depth

e

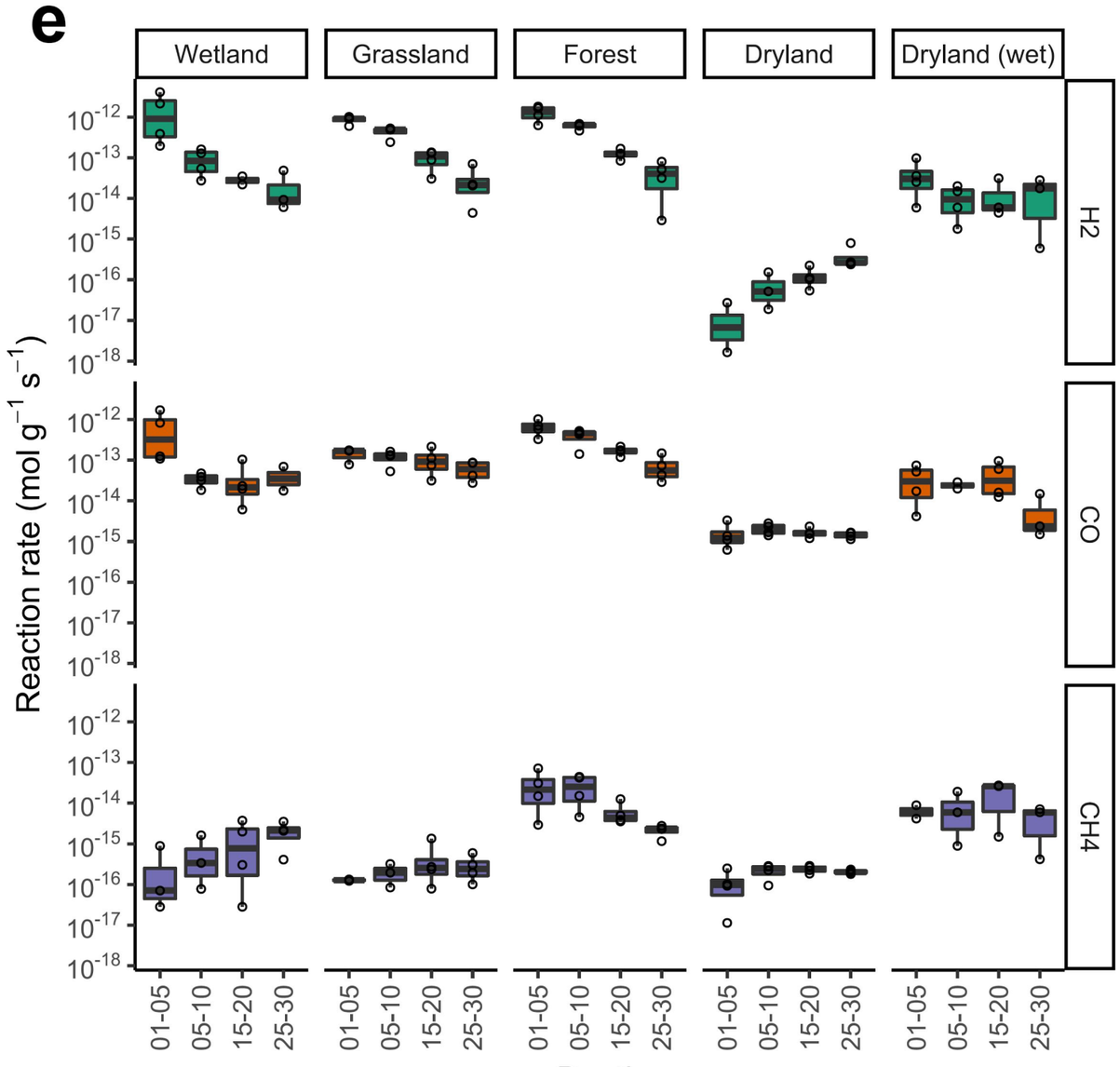
Wetland
Grassland
Forest
Dryland
Dryland (wet)
H2
CO
CH4
Reaction rate (mol g^{-1} s^{-1})
10^{-12}
10^{-13}
10^{-14}
10^{-15}
10^{-16}
10^{-17}
10^{-18}
01-05
05-10
15-20
25-30
Depth
Gas
H_2
CO
CH_4

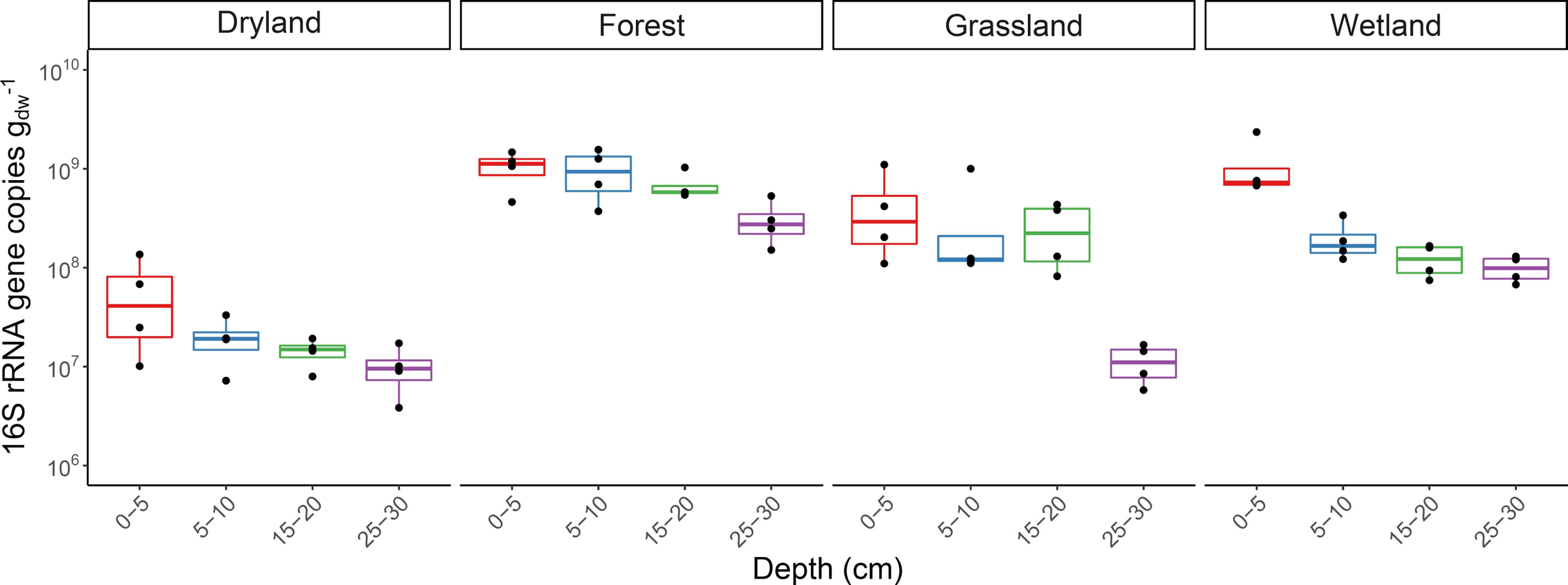
Dryland
Forest
Grassland
Wetland
16S rRNA gene copies g_{dw}^{-1}
10^{10}
10^{9}
10^{8}
10^{7}
10^{6}
0–5
5–10
15–20
25–30
Depth (cm)

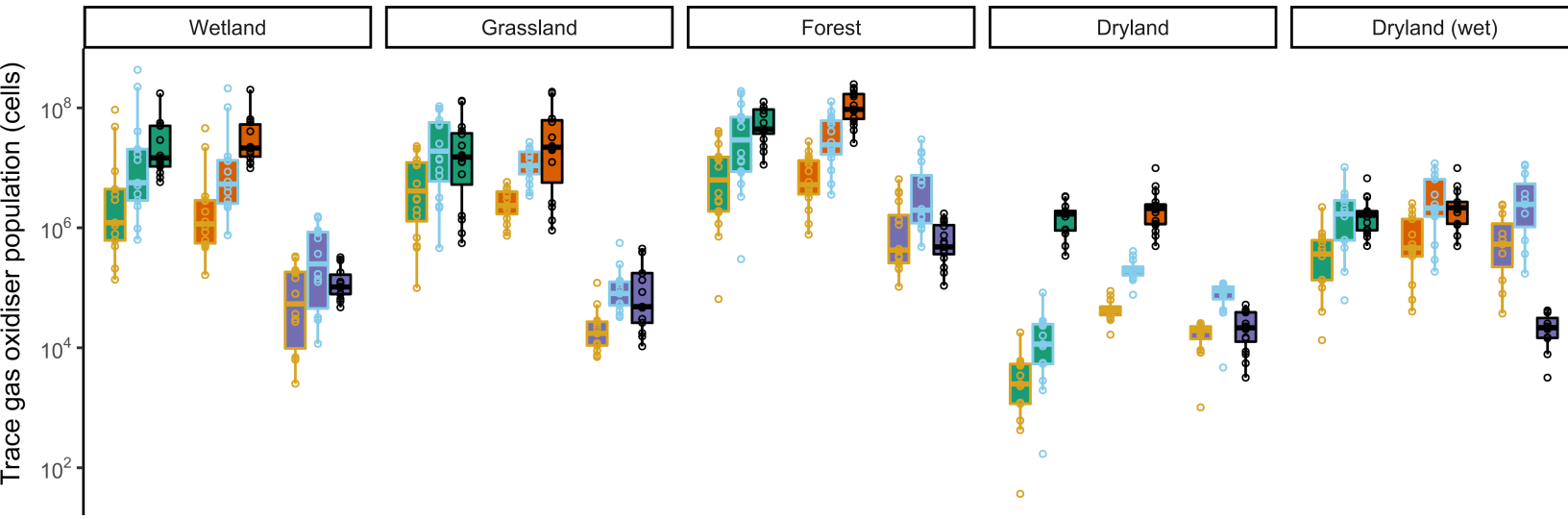
Wetland
Grassland
Forest
Dryland
Dryland (wet)
Trace gas oxidiser population (cells)
10^8
10^6
10^4
10^2

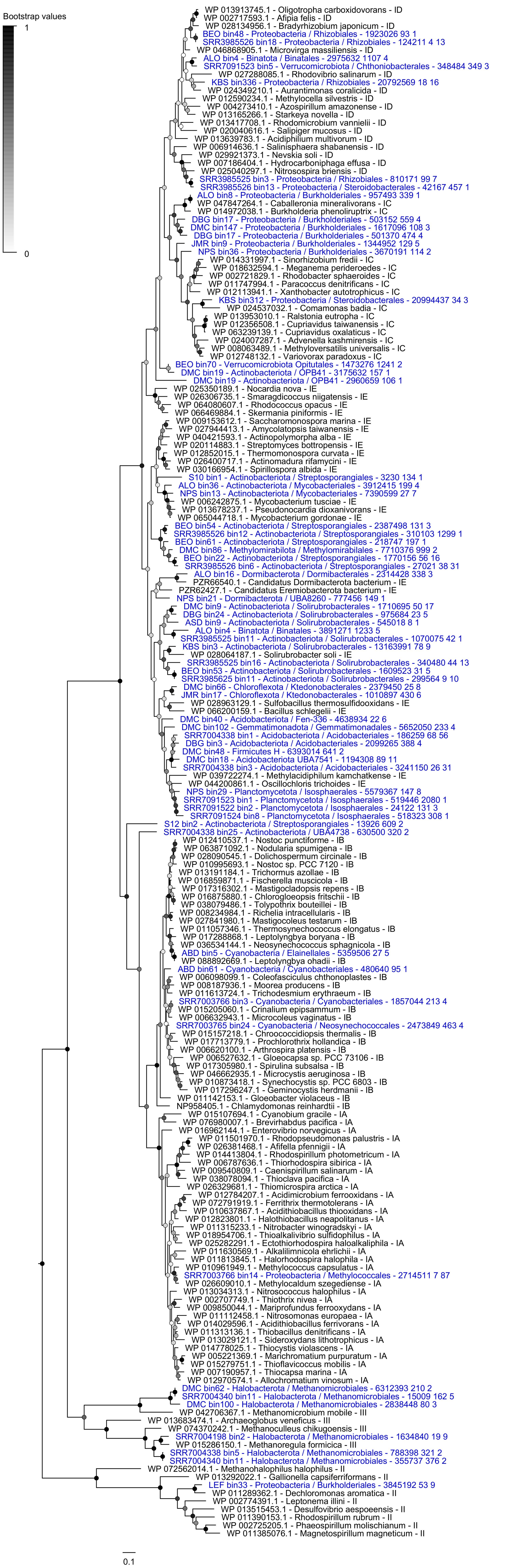
Bootstrap values
1
0
WP 013913745.1 - Oligotropha carboxidovorans - ID
WP 002717593.1 - Afipia felis - ID
WP 028134956.1 - Bradyrhizobium japonicum - ID
BEO bin48 - Proteobacteria / Rhizobiales - 1923026 93 1
SRR3985526 bin18 - Proteobacteria / Rhizobiales - 124211 4 13
WP 046868905.1 - Microvirga massiliensis - ID
ALO bin4 - Binatota / Binatales - 2975632 1107 4
SRR7091523 bin5 - Verrucomicrobiota / Chthoniobacterales - 348484 349 3
WP 027288085.1 - Rhodovibrio salinarum - ID
KBS bin336 - Proteobacteria / Rhizobiales - 20792569 18 16
WP 024349210.1 - Aurantimonas coralicida - ID
WP 012590234.1 - Methylocella silvestris - ID
WP 004273410.1 - Azospirillum amazonense - ID
WP 013165266.1 - Starkeya novella - ID
WP 013417708.1 - Rhodomicrobium vannielii - ID
WP 020040616.1 - Salipiger mucosus - ID
WP 013639783.1 - Acidiphilium multivorum - ID
WP 006914636.1 - Salinisphaera shabanensis - ID
WP 029921373.1 - Nevskia soli - ID
WP 007186404.1 - Hydrocarboniphaga effusa - ID
WP 025040297.1 - Nitrosospira briensis - ID
SRR3985525 bin3 - Proteobacteria / Rhizobiales - 810171 99 7
SRR3985526 bin13 - Proteobacteria / Steroidobacterales - 42167 457 1
ALO bin8 - Proteobacteria / Burkholderiales - 957493 339 1
WP 047847264.1 - Caballeronia mineralivorans - IC
WP 014972038.1 - Burkholderia phenoliruptrix - IC
DBG bin17 - Proteobacteria / Burkholderiales - 503152 559 4
DMC bin147 - Proteobacteria / Burkholderiales - 1617096 108 3
DBG bin17 - Proteobacteria / Burkholderiales - 501370 474 4
JMR bin9 - Proteobacteria / Burkholderiales - 1344952 129 5
NPS bin36 - Proteobacteria / Burkholderiales - 3670191 114 2
WP 014331997.1 - Sinorhizobium fredii - IC
WP 018632594.1 - Meganema perideroedes - IC
WP 002721829.1 - Rhodobacter sphaeroides - IC
WP 011747994.1 - Paracoccus denitrificans - IC
WP 012113941.1 - Xanthobacter autotrophicus - IC
KBS bin312 - Proteobacteria / Steroidobacterales - 20994437 34 3
WP 024537032.1 - Comamonas badia - IC
WP 013953010.1 - Ralstonia eutropha - IC
WP 012356508.1 - Cupriavidus taiwanensis - IC
WP 063239139.1 - Cupriavidus oxalaticus - IC
WP 024007287.1 - Advenella kashmirensis - IC
WP 008063489.1 - Methyloversatilis universalis - IC
WP 012748132.1 - Variovorax paradoxus - IC
BEO bin70 - Verrucomicrobiota Opitutales - 1473276 1241 2
DMC bin19 - Actinobacteriota / OPB41 - 3175632 157 1
DMC bin19 - Actinobacteriota / OPB41 - 2960659 106 1
WP 025350189.1 - Nocardia nova - IE
WP 026306735.1 - Smaragdicoccus niigatensis - IE
WP 064080607.1 - Rhodococcus opacus - IE
WP 066469884.1 - Skermania piniformis - IE
WP 009153612.1 - Saccharomonospora marina - IE
WP 027944413.1 - Amycolatopsis taiwanensis - IE
WP 040421593.1 - Actinopolymorpha alba - IE
WP 020114883.1 - Streptomyces bottropensis - IE
WP 012852015.1 - Thermomonospora curvata - IE
WP 026400717.1 - Actinomadura rifamycini - IE
WP 030166954.1 - Spirillospora albida - IE
S10 bin1 - Actinobacteriota / Streptosporangiales - 3230 134 1
ALO bin36 - Actinobacteriota / Mycobacteriales - 3912415 199 4
NPS bin13 - Actinobacteriota / Mycobacteriales - 7390599 27 7
WP 006242875.1 - Mycobacterium tusciae - IE
WP 013678237.1 - Pseudonocardia dioxanivorans - IE
WP 065044718.1 - Mycobacterium gordonae - IE
BEO bin54 - Actinobacteriota / Streptosporangiales - 2387498 131 3
SRR3985526 bin12 - Actinobacteriota / Streptosporangiales - 310103 1299 1
BEO bin61 - Actinobacteriota / Streptosporangiales - 218747 197 1
DMC bin86 - Methylomirabilota / Methylomirabilales - 7710376 999 2
BEO bin22 - Actinobacteriota / Streptosporangiales - 1770156 56 16
SRR3985526 bin6 - Actinobacteriota / Streptosporangiales - 27021 38 31
ALO bin16 - Dormibacterota / Dormibacterales - 2314428 338 3
PZR66540.1 - Candidatus Dormibacterota bacterium - IE
PZR62427.1 - Candidatus Eremiobacterota bacterium - IE
NPS bin21 - Dormibacterota / UBA8260 - 777456 149 1
DMC bin9 - Actinobacteriota / Solirubrobacterales - 1710695 50 17
DBG bin24 - Actinobacteriota / Solirubrobacterales - 975684 23 5
ASD bin9 - Actinobacteriota / Solirubrobacterales - 545018 8 1
ALO bin4 - Binatota / Binatales - 3891271 1233 5
SRR3985525 bin11 - Actinobacteriota / Solirubrobacterales - 1070075 42 1
KBS bin3 - Actinobacteriota / Solirubrobacterales - 13163991 78 9
WP 028064187.1 - Solirubrobacter soli - IE
SRR3985525 bin16 - Actinobacteriota / Solirubrobacterales - 340480 44 13
BEO bin53 - Actinobacteriota / Solirubrobacterales - 1609523 31 5
SRR3985625 bin11 - Actinobacteriota / Solirubrobacterales - 299564 9 10
DMC bin66 - Chloroflexota / Ktedonobacterales - 2379450 25 8
JMR bin17 - Chloroflexota / Ktedonobacterales - 1010897 430 6
WP 028963129.1 - Sulfobacillus thermosulfidooxidans - IE
WP 066200159.1 - Bacillus schlegelii - IE
DMC bin40 - Acidobacteriota / Fen-336 - 4638934 22 6
DMC bin102 - Gemmatimonadota / Gemmatimonadales - 5652050 233 4
SRR7004338 bin1 - Acidobacteriota / Acidobacteriales - 186259 68 56
DBG bin3 - Acidobacteriota / Acidobacteriales - 2099265 388 4
DMC bin48 - Firmicutes H - 6393014 641 2
DMC bin18 - Acidobacteriota UBA7541 - 1194308 89 11
SRR7004338 bin3 - Acidobacteriota / Acidobacteriales - 3241150 26 31
WP 039722274.1 - Methylacidiphilum kamchatkense - IE
WP 044200861.1 - Oscillochloris trichoides - IE
NPS bin29 - Planctomycetota / Isosphaerales - 5579367 147 8
SRR7091523 bin1 - Planctomycetota / Isosphaerales - 519446 2080 1
SRR7091522 bin2 - Planctomycetota / Isosphaerales - 24122 131 3
SRR7091524 bin8 - Planctomycetota / Isosphaerales - 518323 308 1
S12 bin2 - Actinobacteriota / Streptosporangiales - 13926 609 2
SRR7004338 bin25 - Actinobacteriota / UBA4738 - 630500 320 2
WP 012410537.1 - Nostoc punctiforme - IB
WP 063871092.1 - Nodularia spumigena - IB
WP 028090545.1 - Dolichospermum circinale - IB
WP 010995693.1 - Nostoc sp. PCC 7120 - IB
WP 013191184.1 - Trichormus azollae - IB
WP 016859871.1 - Fischerella muscicola - IB
WP 017316302.1 - Mastigocladopsis repens - IB
WP 016875880.1 - Chlorogloeopsis fritschii - IB
WP 038079486.1 - Tolypothrix bouteillei - IB
WP 008234984.1 - Richelia intracellularis - IB
WP 027841980.1 - Mastigocoleus testarum - IB
WP 011057346.1 - Thermosynechococcus elongatus - IB
WP 017288868.1 - Leptolyngbya boryana - IB
WP 036534144.1 - Neosynechococcus sphagnicola - IB
ABD bin5 - Cyanobacteria / Elainellales - 5359506 27 5
WP 088892669.1 - Leptolyngbya ohadii - IB
ABD bin61 - Cyanobacteria / Cyanobacteriales - 480640 95 1
WP 006098099.1 - Coleofasciculus chthonoplastes - IB
WP 008187936.1 - Moorea producens - IB
WP 011613724.1 - Trichodesmium erythraeum - IB
SRR7003766 bin3 - Cyanobacteria / Cyanobacteriales - 1857044 213 4
WP 015205060.1 - Crinalium epipsammum - IB
WP 006632943.1 - Microcoleus vaginatus - IB
SRR7003765 bin24 - Cyanobacteria / Neosynechococcales - 2473849 463 4
WP 015157218.1 - Chroococcidiopsis thermalis - IB
WP 017713779.1 - Prochlorothrix hollandica - IB
WP 006620100.1 - Arthrospira platensis - IB
WP 006527632.1 - Gloeocapsa sp. PCC 73106 - IB
WP 017305980.1 - Spirulina subsalsa - IB
WP 046662935.1 - Microcystis aeruginosa - IB
WP 010873418.1 - Synechocystis sp. PCC 6803 - IB
WP 017296247.1 - Geminocystis herdmanii - IB
WP 011142153.1 - Gloeobacter violaceus - IB
NP958405.1 - Chlamydomonas reinhardtii - IB
WP 015107694.1 - Cyanobium gracile - IA
WP 076980007.1 - Brevirhabdus pacifica - IA
WP 016962144.1 - Enterovibrio norvegicus - IA
WP 011501970.1 - Rhodopseudomonas palustris - IA
WP 026381468.1 - Afifella pfennigii - IA
WP 014413804.1 - Rhodospirillum photometricum - IA
WP 006787636.1 - Thiorhodospira sibirica - IA
WP 009540809.1 - Caenispirillum salinarum - IA
WP 038078094.1 - Thioclava pacifica - IA
WP 026329681.1 - Thiomicrospira arctica - IA
WP 012784207.1 - Acidimicrobium ferrooxidans - IA
WP 072791919.1 - Ferrithrix thermotolerans - IA
WP 010637867.1 - Acidithiobacillus thiooxidans - IA
WP 012823801.1 - Halothiobacillus neapolitanus - IA
WP 011315233.1 - Nitrobacter winogradskyi - IA
WP 018954706.1 - Thioalkalivibrio sulfidophilus - IA
WP 025282291.1 - Ectothiorhodospira haloalkaliphila - IA
WP 011630569.1 - Alkalilimnicola ehrlichii - IA
WP 011813845.1 - Halorhodospira halophila - IA
WP 010961949.1 - Methylococcus capsulatus - IA
SRR7003766 bin14 - Proteobacteria / Methylococcales - 2714511 7 87
WP 026609010.1 - Methylocaldum szegediense - IA
WP 013034313.1 - Nitrosococcus halophilus - IA
WP 002707749.1 - Thiothrix nivea - IA
WP 009850044.1 - Mariprofundus ferrooxydans - IA
WP 011112458.1 - Nitrosomonas europaea - IA
WP 014029596.1 - Acidithiobacillus ferrivorans - IA
WP 011313136.1 - Thiobacillus denitrificans - IA
WP 013029121.1 - Sideroxydans lithotrophicus - IA
WP 014778025.1 - Thiocystis violascens - IA
WP 005221369.1 - Marichromatium purpuratum - IA
WP 015279751.1 - Thioflavicoccus mobilis - IA
WP 007190957.1 - Thiocapsa marina - IA
WP 012970574.1 - Allochromatium vinosum - IA
DMC bin62 - Halobacterota / Methanomicrobiales - 6312393 210 2
SRR7004340 bin11 - Halobacterota / Methanomicrobiales - 15009 162 5
DMC bin100 - Halobacterota / Methanomicrobiales - 2838448 80 3
WP 042706367.1 - Methanomicrobium mobile - III
WP 013683474.1 - Archaeoglobus veneficus - III
WP 074370242.1 - Methanoculleus chikugoensis - III
SRR7004198 bin2 - Halobacterota / Methanomicrobiales - 1634840 19 9
WP 015286150.1 - Methanoregula formicica - III
SRR7004338 bin5 - Halobacterota / Methanomicrobiales - 788398 321 2
SRR7004340 bin11 - Halobacterota / Methanomicrobiales - 355737 376 2
WP 072562014.1 - Methanohalophilus halophilus - II
WP 013292022.1 - Gallionella capsiferriformans - II
LEF bin33 - Proteobacteria / Burkholderiales - 3845192 53 9
WP 011289362.1 - Dechloromonas aromatica - II
WP 002774391.1 - Leptonema illini - II
WP 013515453.1 - Desulfovibrio aespoeensis - II
WP 011390153.1 - Rhodospirillum rubrum - II
WP 002725205.1 - Phaeospirillum molischianum - II
WP 011385076.1 - Magnetospirillum magneticum - II
0.1

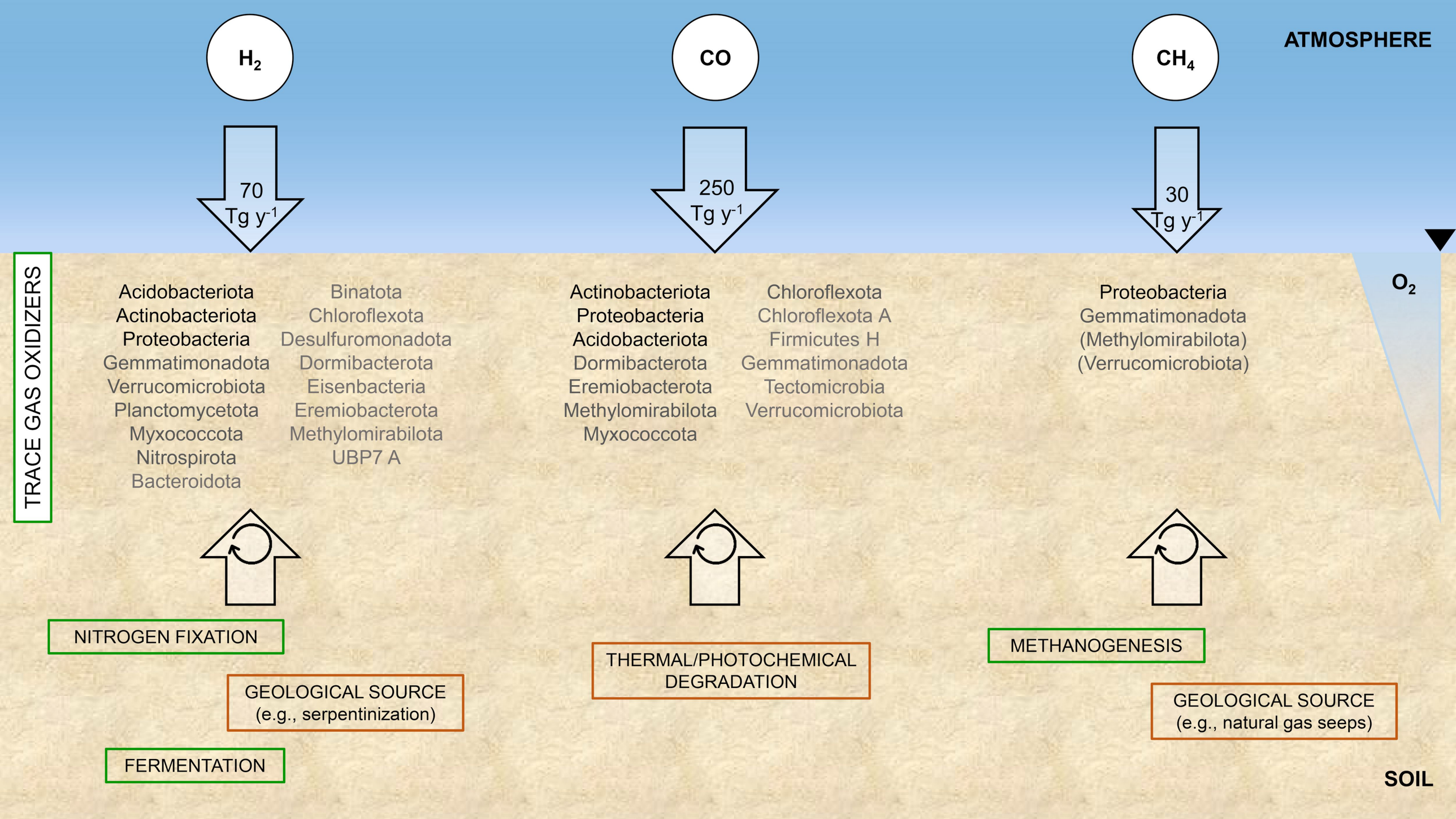
ATMOSPHERE
H_2
CO
CH_4
70 Tg y^{-1}
250 Tg y^{-1}
30 Tg y^{-1}
O_2
TRACE GAS OXIDIZERS
Acidobacteriota
Actinobacteriota
Proteobacteria
Gemmatimonadota
Verrucomicrobiota
Planctomycetota
Myxococcota
Nitrospirota
Bacteroidota
Binatota
Chloroflexota
Desulfuromonadota
Dormibacterota
Eisenbacteria
Eremiobacterota
Methylomirabilota
UBP7 A
Actinobacteriota
Proteobacteria
Acidobacteriota
Dormibacterota
Eremiobacterota
Methylomirabilota
Myxococcota
Chloroflexota
Chloroflexota A
Firmicutes H
Gemmatimonadota
Tectomicrobia
Verrucomicrobiota
Proteobacteria
Gemmatimonadota
(Methylomirabilota)
(Verrucomicrobiota)
NITROGEN FIXATION
GEOLOGICAL SOURCE
(e.g., serpentinization)
FERMENTATION
THERMAL/PHOTOCHEMICAL
DEGRADATION
METHANOGENESIS
GEOLOGICAL SOURCE
(e.g., natural gas seeps)
SOIL